

Chapter 7

Molecular Dynamics Studies of Calcium Fluoride

7.1 Introduction

Molecular Dynamics (MD) studies are the most direct way of predicting the effect of temperature on the atomistic behaviour of ionic solids. One particular aspect where MD can prove particularly useful are studies of melting and evaporation [49, 50, 130]. However, since these occur on an exceptionally fast time scale they are very difficult to monitor experimentally. Thus MD simulations can provide valuable information about the atomic processes involved during these events. In the present chapter two different sized nano-clusters are studied in an attempt to model the melting and solidification of CaF_2 . In addition, we use the nano-clusters to study surface relaxation as a function of surface size by comparing the relaxation of the surface ions on the two nano-clusters (which clearly have finite surface areas), with the relaxation of an infinite two dimensional surface.

CaF_2 was chosen as it is isostructural with CeO_2 , but since it is highly ionic, the MD simulations can be used with a greater degree of confidence, as at present PENICILLIN is unable to incorporate shell model polarisabilities. Nevertheless, inferences can still be made from the present study to the behaviour of CeO_2 . For example, by comparing the present 3D dynamic model with the results from the 2D static simulations, we may be able to add weight to the conclusions on surface structure and crystal morphologies derived from the 2D simulations of CeO_2 .

7.2 Methodology

7.2.1 Simulation Techniques

The infinite 2D surface simulations of CaF_2 were carried out using the MARVIN code. This relaxes the surface by Newton-Rhapson and conjugate minimisation techniques. A more detailed discussion of the methodology can be found in Chapter 2.

The molecular dynamics (MD) studies were carried out with the PENICILLIN code. Two different nano-clusters were studied to examine the finite surface relaxation; a large 3645 atom cluster and a smaller 1665 atom cluster. The latter cluster was additionally used in studies of melting and solidification. The initial starting geometries of the clusters were chosen such that their morphologies were as close as possible to being spherical, while using only low index faces. In practical terms, such a morphology ensures the variation of the electric field around the cluster is not too dramatic. This prevents ions at low coordinate sites from acquiring too much energy and leaving the cluster. Although there is presently no way of choosing an optimum geometry systematically, a suitable geometry for both clusters was found to be an

octahedron (a (111) surface dominated morphology) with large (200) surface facets cut onto it.

7.2.2 Potential Parameters

The potentials in the present study, use a modified Buckingham potential. In addition, to the r^{-6} term, an r^{-12} term is also added, this additional term prevents the ions falling into the Buckingham short range energy well that arises as a result of the r^{-6} term (Figure 7.1). Hence the potential has the form,

$$S_{ij} = A \exp\left(\frac{-r_{ij}}{\rho}\right) - \frac{C}{r_{ij}^6} + \frac{D}{r_{ij}^{12}} \quad (7.1)$$

Such D-terms are not used in static minimisation studies as the ions rarely relax very far from their equilibrium positions. However, in non-equilibrium dynamic simulation, especially at high temperatures, it is possible for individual ions to have very high instantaneous energies. Such high energy ions may fall into the infinite negative energy although in the present case this is unlikely as the repulsive energy between 1.1-1.5Å is very high. Nevertheless, the effect on the forces may still be significant. In the present study, $D = C$ for all ion interaction. The potential parameters are listed in Table 7.1, and were derived by Grimes and have been rigorously tested in studies of the bulk and triatomic molecules [50]. The rigid ion model has been used in the present work for the reasons discussed above. The omission of the shells will not greatly affect the results as CaF_2 is a highly ionic solid. Further weight is added to this argument as molecular dynamic studies of MgO which do use the shell model, [49], show its inclusion has little effect on properties such as the melting point. A D-term has been used for the $\text{F}^- - \text{F}^-$ interaction as this has an attractive C-term which

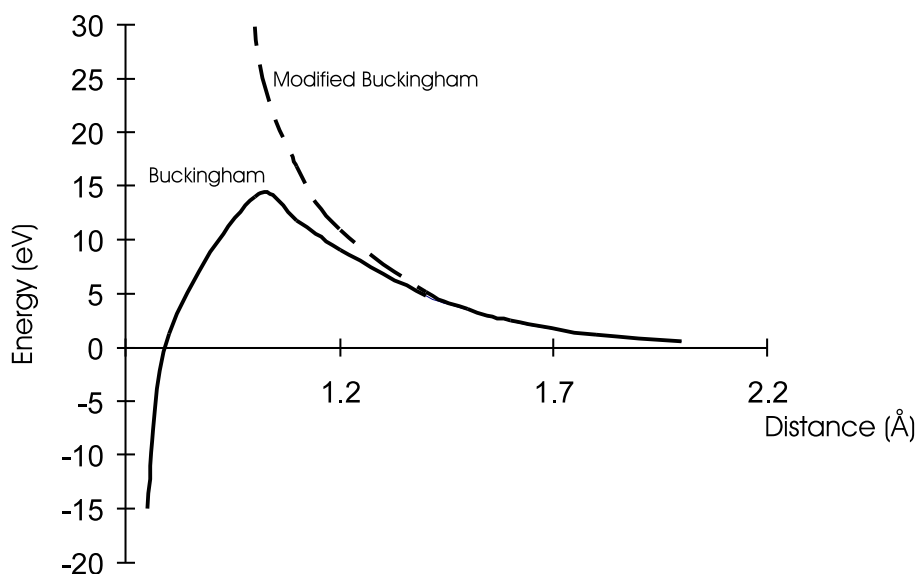


Figure 7.1: The form of the Buckingham potential for the F^- - F^- , with and without the D-term.

may bring the ions close enough to fall into the Buckingham short range energy well. A D-term is not required for the other interactions as no attractive components are present in the short range potential.

Interaction	A(eV)	$\rho(\text{\AA}^{-1})$	C(eV \AA^6)	D(eV \AA^{12})
$\text{Ca}^{2+} - \text{Ca}^{2+}$	44898.1	0.169	0.00	0.00
$\text{Ca}^{2+} - \text{F}^-$	1273.8	0.2997	0.00	0.00
$\text{F}^- - \text{F}^-$	1127.7	0.2753	15.83	15.83

Table 7.1: Potential parameters

7.2.3 α - shapes

Visualisation of the surface relaxation proved to be very difficult using conventional atomic models as too many atoms were present in the cluster to develop an overall view of relaxation. An overall picture can be developed by using a visualisation

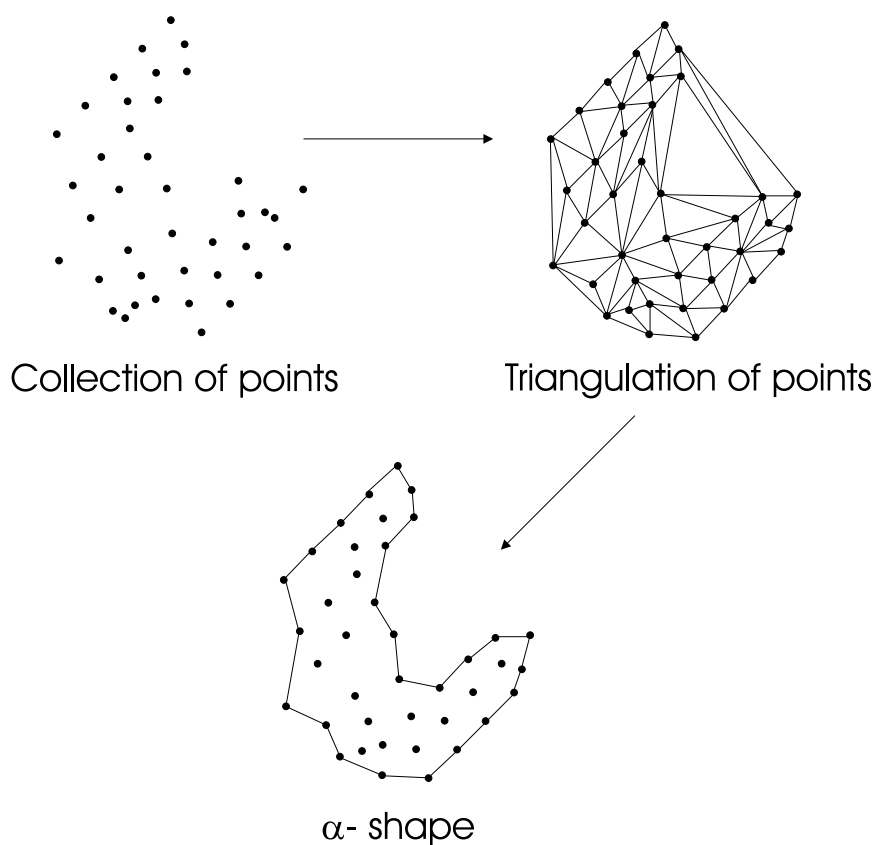


Figure 7.2: Formation of a 2D alpha shape. The shape is formed by the removal of triangle of a specific size after triangulation.

technique known as α - shapes [131]. This entails the representation of the atoms as vertices of tetrahedra. Those tetrahedra which are larger than a given radius are removed. A two dimensional example is shown in Figure 7.2. The resulting shape (the α - shape) captures the ‘intuitive’ form of the cluster. The technique is analogous to using polyhedra to represent SiO_4^{2-} units in silicious material or using spacefilling diagrams to represent the electron clouds of molecules.

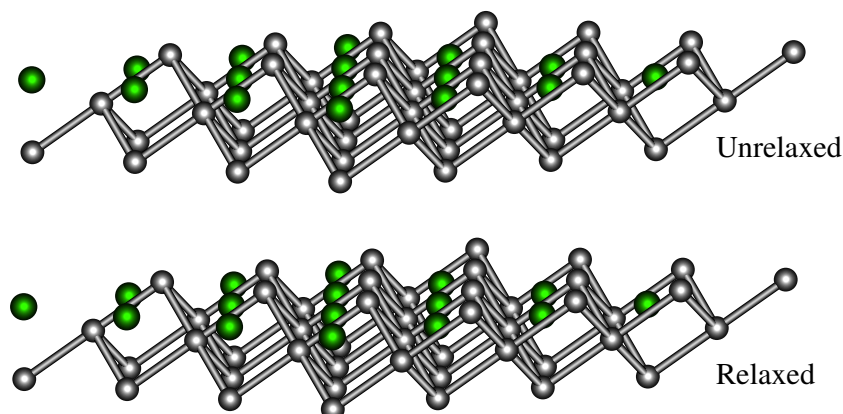


Figure 7.3: Surface structure of the (111) faces

7.3 Surface relaxation; comparison of finite and infinite systems

7.3.1 Two dimensional surface simulations: gradient minimisation

111 - As with the previous studies of the (111) surface in CeO_2 , the calcium fluoride surface shows very little relaxation (Figure 7.3) as all the ions are symmetrically coordinated. The surface is also thermodynamically very stable (Table 7.2).

200 - This is a type III surface and can be stabilised by either creating F^- interstitials or Ca^{2+} vacancies on a Ca^{2+} terminated surface. Additionally, the two F^- ions can be arranged in two possible ways; either diagonally to each other or next to one another. Table 7.2 and Figure 7.4 show the energetics and surface structure of such systems. The most thermodynamically stable configuration on the (200) surface is

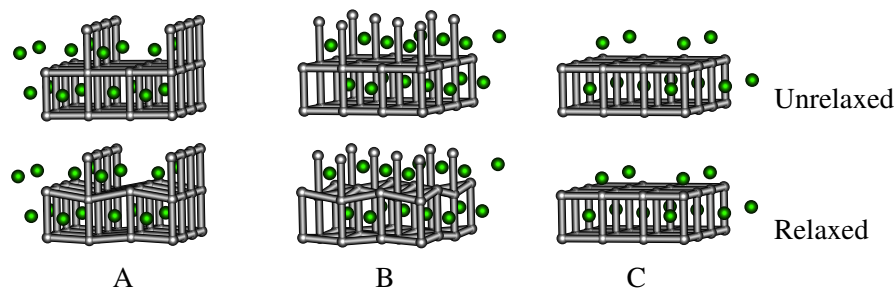


Figure 7.4: Surface structure of the (200) faces

Surface	Configuration	Unrelaxed	Relaxed
(111)	0.5	0.51	0.49
(200)	0.125 (A)	2.40	1.37
	0.125 (B)	1.71	0.99
	0.375 (C)	3.08	1.83

Table 7.2: Surface energies (in Jm^{-2})

where the defects are anions which are arranged diagonally opposite to each other (Configuration B), this is analogous to the results for CeO_2 .

7.3.2 MD relaxation of the 3656 atom cluster

The relaxation of this finite cluster, shows some similarities with the results from the MARVIN simulations. However, the finite nature of the surfaces is also evident for this cluster. In the present study we use α -shape analysis. Their use has the advantage of clearly showing small changes in the overall surface structure, such detail is easily obscured in figures of atoms. The lighter colours are due to the calcium tetrahedra, while the darker colours are due to the fluorine tetrahedra. Thus, the lighter coloured areas in the alpha shapes are where the calcium tetrahedra are at the surface and

the dark areas are where fluorine atoms are at the surface. Additionally, in areas where both dark and light colours are present the relative heights between the colours represents the relative heights between the tetrahedra. The accuracy of the technique is discussed at the end of the present section.

The pairs of figures, 7.5 and 7.6, 7.7 and 7.8, 7.9 and 7.10 show the cluster before and after it has equilibrated at 10K for 35ps. In the orientation of Figures 7.5 and 7.6, two (200) faces and two (111) faces are visible. The two (111) faces show a fairly uniform relaxation similar to that seen in the 2D infinite surface simulations. However, the ions at the edges of the surface are slightly higher than those in the centre and form ridge like structures. This is a result of these ions not being as symmetrically coordinated compared with those ions at the centre of the face.

The Ca^{2+} terminated (200) face after relaxation shows the presence of F^- interstitial ions, represented by the presence of darker colours on the surface, this is seen most clearly in Figure 7.6 and 7.10. The ions seem to show some degree of ordering hence the ‘criss-cross’ pattern. The nature of the ordering is reminiscent of the lowest surface energy arrangement of the F^- ions in the MARVIN simulations, with the anions being diagonally opposite to each other. Clearly, these defects have formed to counter the dipole of the type III surface despite the relatively small thickness of the crystallite. This vindicates the approach used in the MARVIN calculations for the stabilisation of the type III surfaces. In addition, it supports the conclusions made in the previous chapter, from infinite surface simulations, that cation terminated surfaces are unfavourable due to their high charge density.

The F^- terminated (200) surface (at the bottom of the cluster), shows the presence of F^- vacancies (the exposure of the lighter calcium areas). These particular vacancies

do not show the same degree of ordering as those on the previous face discussed. This may be a result of the equilibration time being too short for the energy differences between the two ordering types (i.e. Configurations A and B) to become apparent. Figures 7.7 and 7.8 show the best views of a fluorine terminated (200) surface.

One point of note is that the ridge between the two (111) faces in Figure 7.5 is covered by anions after relaxation (Figure 7.6). Such behaviour is the result of Ca^{2+} ions not being favourable at the surface. In addition, the sharp boundary that existed between the (111) and (200) face (Figures 7.6, 7.8 and 7.10) have become more rounded, but still remain easily identifiable.

In Figures 7.9 and 7.10 three unique edges are visible: a triple point where two (111) and (200) faces met, the edge between two (111) faces, and an edge between (111) and (200) faces. After relaxation, all the edges seen are covered by F^- ions. The two triple points are still discernible, however, their angularity has decreased, with the corners becoming more rounded and the cluster looking slightly more spherical. The edges also show a relaxation and lose their sharpness, however they still remain relatively well defined.

To ensure that the conclusions made from the alpha shape representations are a reflections of the ‘real’ atomic behaviour and not a consequence of the method of making diagrams, the atomic structures of a cross section of the cluster is shown in Figures 7.11. The diagram confirms the conclusions made using the alpha clusters. After relaxation, one sees the formation of F^- interstitials ions on the calcium terminated surface and F^- vacancies on the fluorine terminated surface.

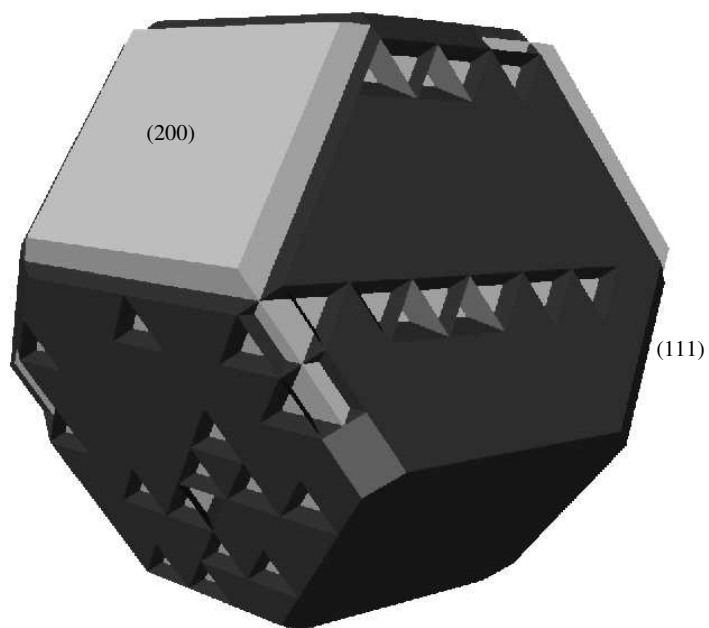


Figure 7.5: Unrelaxed



Figure 7.6: Relaxed

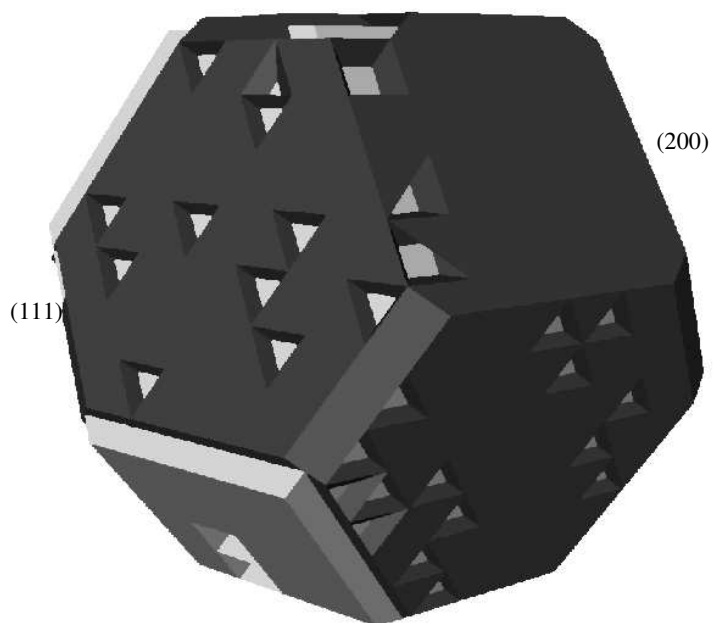


Figure 7.7: Unrelaxed

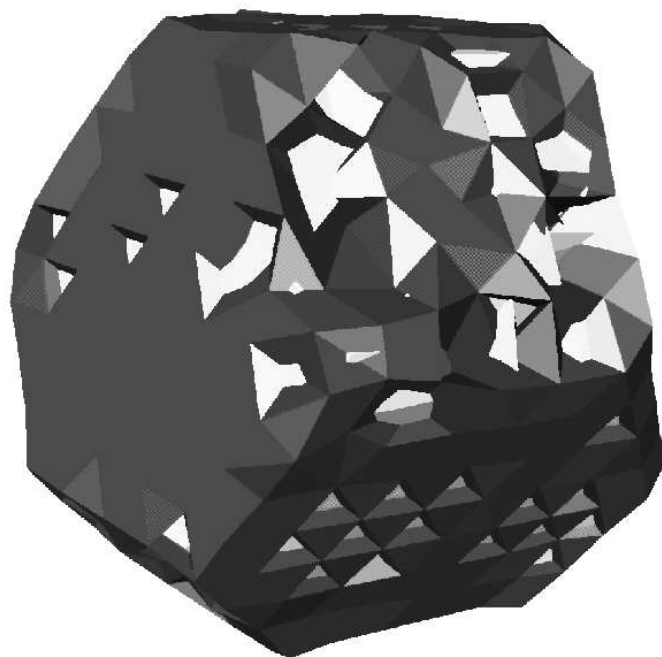


Figure 7.8: Relaxed

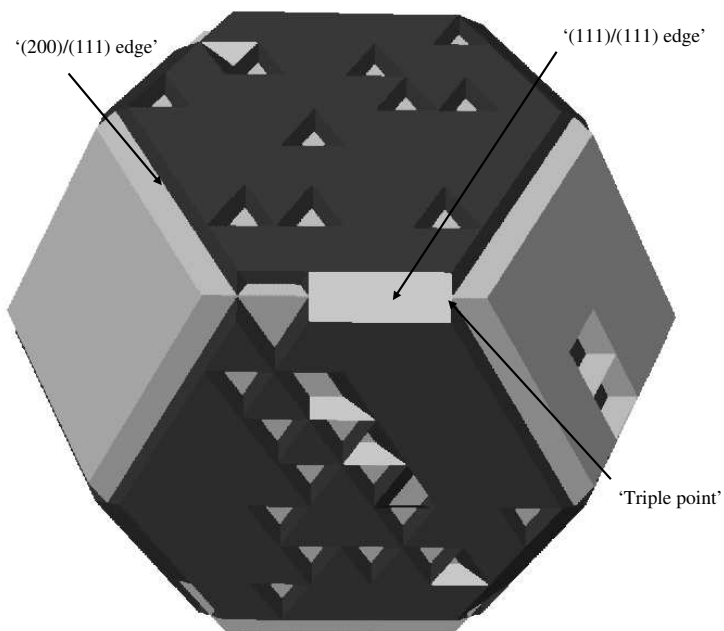


Figure 7.9: Unrelaxed

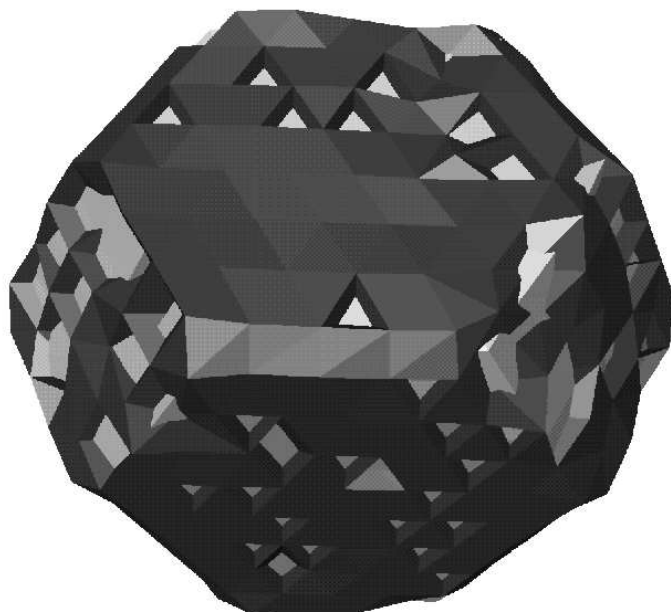


Figure 7.10: Relaxed

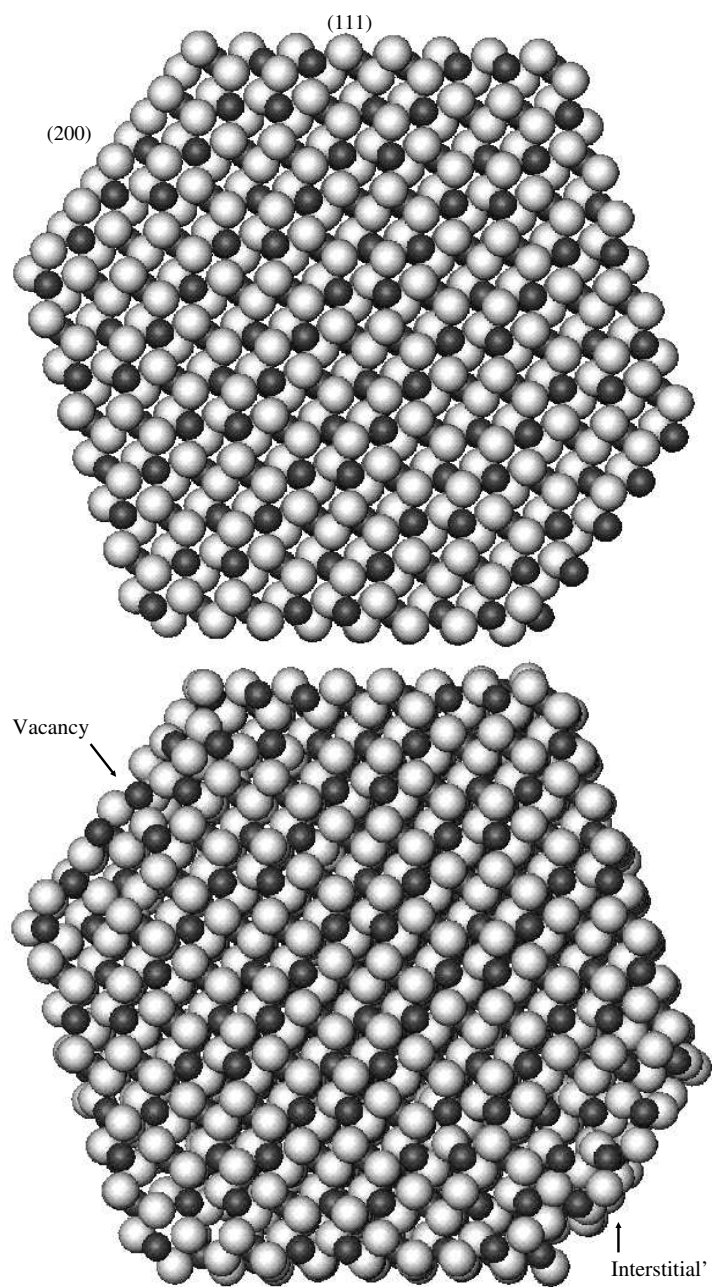


Figure 7.11: Atomic cross section of the 3656 atom cluster. Top - Unrelaxed, Bottom - Relaxed

7.3.3 MD relaxation of 1665 atom cluster

This cluster has a much larger surface/bulk ratio, hence the relaxation it shows is more extreme. Consequently, it bears less resemblance to the infinite surface calculations than the larger cluster does. However, there are still some similarities with the infinite surface simulations.

Figures 7.12 and 7.13 show the intersection of three unrelaxed faces: two (111) faces and a (200) face. When the (111) faces have relaxed, like their infinite surface counterparts they show very little atomic rearrangement on the surface. There is however, a slight depression in the centre of the (111) face. However, the ions at the edge of the surface which are not subject to such forces, show a different and more extreme relaxation than their counterparts in the larger cluster.

Although the centre of the (111) surface shows no significant relaxation, the ‘triple point’ where the two (111) and (200) faces meet shows a marked rearrangement; a substantial part of the (200) face and a smaller amount of the (111) face seen have effectively merged together. This obliterates the sharp corner seen in the unrelaxed cluster resulting in the formation of a more rounded cluster. The remaining (200) face in the present picture also shows a heavy relaxation.

Figures 7.14 and 7.15 show a direct view of a (200) face. Like the larger cluster, this surface shows the formation of F^- vacancies. In addition, this particular (200) face shows a ‘bowing out’; where the edges of the face bend outwards to form an oval shaped face. This reduces the number of sharp edges which tend to exhibit large electric fields and are thus not very favourable.

Figures 7.16 and 7.17 show two of the (111) faces and two (200) faces. However, unlike the previous (200) faces discussed, these faces are Ca^{2+} terminated. The

principal observation is that upon relaxation (Figure 7.17) this cation terminated type III surface is stabilised by the presence of F^- interstitial ions, which must have migrated from other areas of the cluster. Furthermore, the diagram shows some evidence that the (111) faces bow inwards at the centre of face. Such a depression, corresponds to the slight downward movement of all the (111) surface ions in the two dimensional surface calculations. However, as the surface is finite, only the symmetric atoms at the surface centre are able to relax in this manner. The atoms at the edges of the surface relax to form flat ridges.

Figure 7.18 shows an atomic cross section for the smaller cluster, before and after relaxation. Again, as with the larger cluster these diagrams support the conclusions made from the alpha-shape representations. The diagram shows evidence of type III surface stabilisation and additionally shows the bowing of the surface and the rounding of the corners

Overall, the smaller cluster attempts to rearrange to form a more spherical shape, with substantial relaxation in some areas. This would be expected given the ratio of surface ions to bulk ions. However, it does show some similarities with the infinite surface model, such as the stabilisation of type III surfaces by F^- interstitial ions. The larger cluster shows an intermediate behaviour between these extremes, such as the (111) surface relaxation being very similar to that of the MARVIN results and some evidence of interstitial defect ordering on some of the type III faces. However, the finite nature of the surfaces also influences the relaxation, such as in the ‘rounding’ at the edges. Nevertheless, the rearrangements are not as drastic as those seen in the smaller cluster.

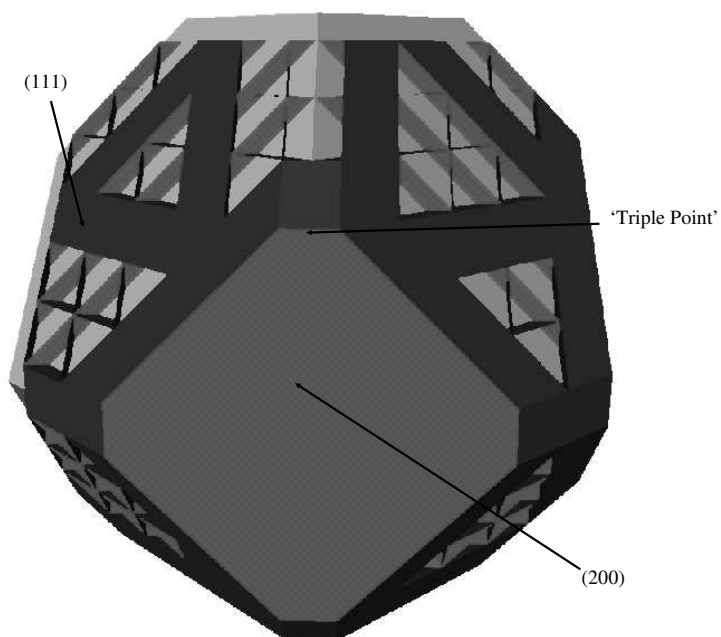


Figure 7.12: Unrelaxed



Figure 7.13: Relaxed

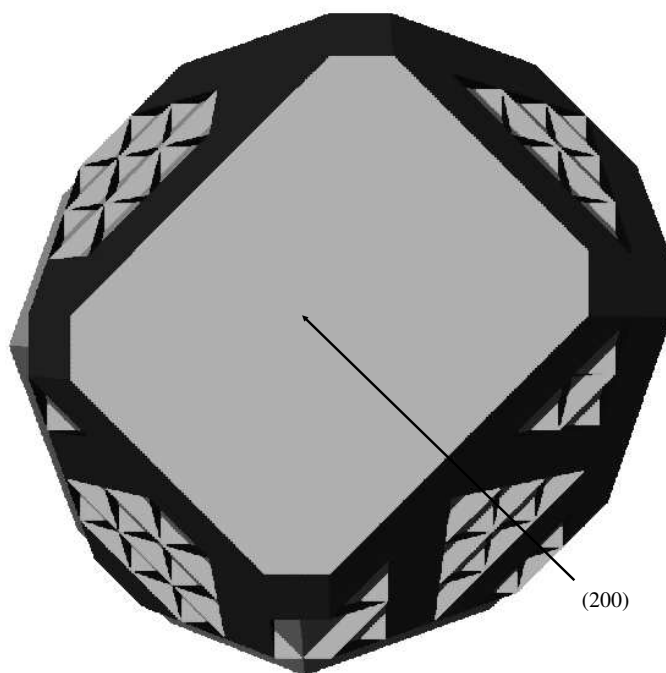


Figure 7.14: Unrelaxed



Figure 7.15: Relaxed

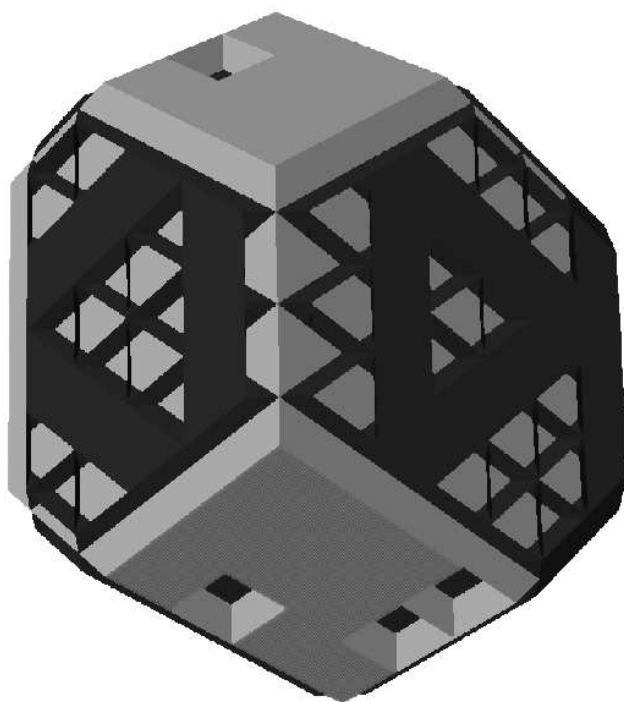


Figure 7.16: Unrelaxed



Figure 7.17: Relaxed

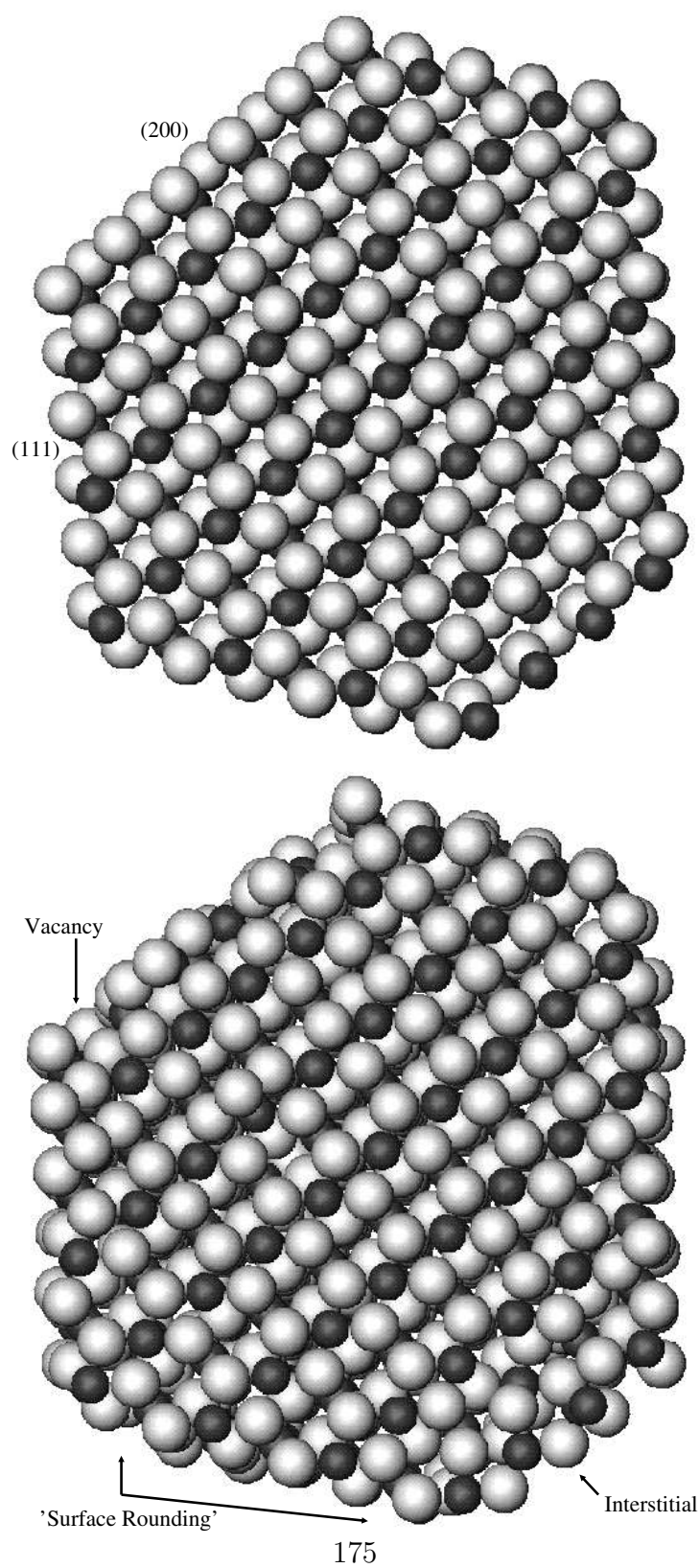


Figure 7.18: Atomic cross section of the 1665 atom cluster. Top - Unrelaxed, Bottom-Relaxed

7.4 The melting of the 1665 atom cluster

Initially, the cluster was allowed to equilibrate for approximately 55ps at 10K, so that it reached its energy minimum and that the correct velocities of all the atoms could be calculated. After this equilibration step, the cluster was heated at a rate of 5K every 100 time steps (i.e. $5 \times 10^{13} \text{Ks}^{-1}$). The thermal history until melting is summarised in Figure 7.19. Figure 7.20 is an expansion of this graph to show the thermal history during the melting process. The heating was stopped when the cluster reached 300K and was allowed to re-equilibrate for ≈ 1 ps, so as to ensure the cluster had fully equilibrated. If the cluster had not been properly equilibrated, the temperature would have continued to rise when the heating was turned off. Once it had been established that there were no problems, heating was resumed at the same rate until the system had melted. During the process, the cluster was analysed by studying both the Fourier transforms of the individual atomic species (which are components of the single crystal diffraction patterns) and also a visual analysis of the atoms in the cluster.

0.0ps This is the unrelaxed cluster and was shown in Figure 7.18. Figures 7.21 and 7.22 show the respective Fourier transforms (FT) for the simple cubic fluorine sub-lattice and the body centred cubic calcium sub-lattice. Both FT's are symmetric and reflect the periodicity of the crystal. The FT's of the fluorine sub-lattice show diffuse scatter intensity due to the finite nature of the cluster. In addition to studying the degree of ordering in the cluster, the FT's permit the calculation of bond distance; from the present patterns the $\text{F}^- - \text{F}^-$ bond distance is 2.73\AA and the $\text{Ca}^{2+} - \text{Ca}^{2+}$ is 5.46\AA which are identical to those seen in a bulk crystal. This is not surprising given

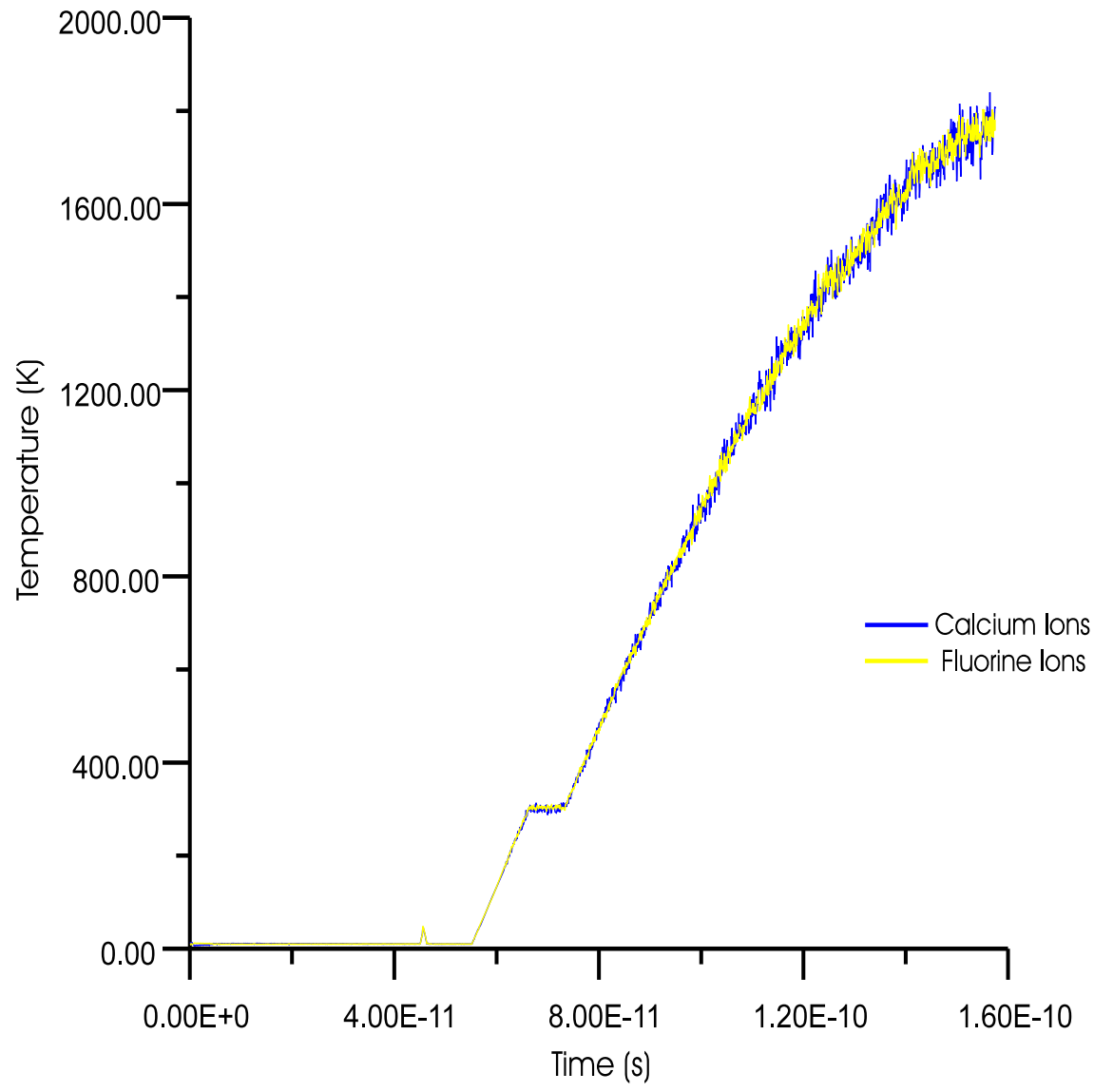


Figure 7.19: Heating history of the cluster

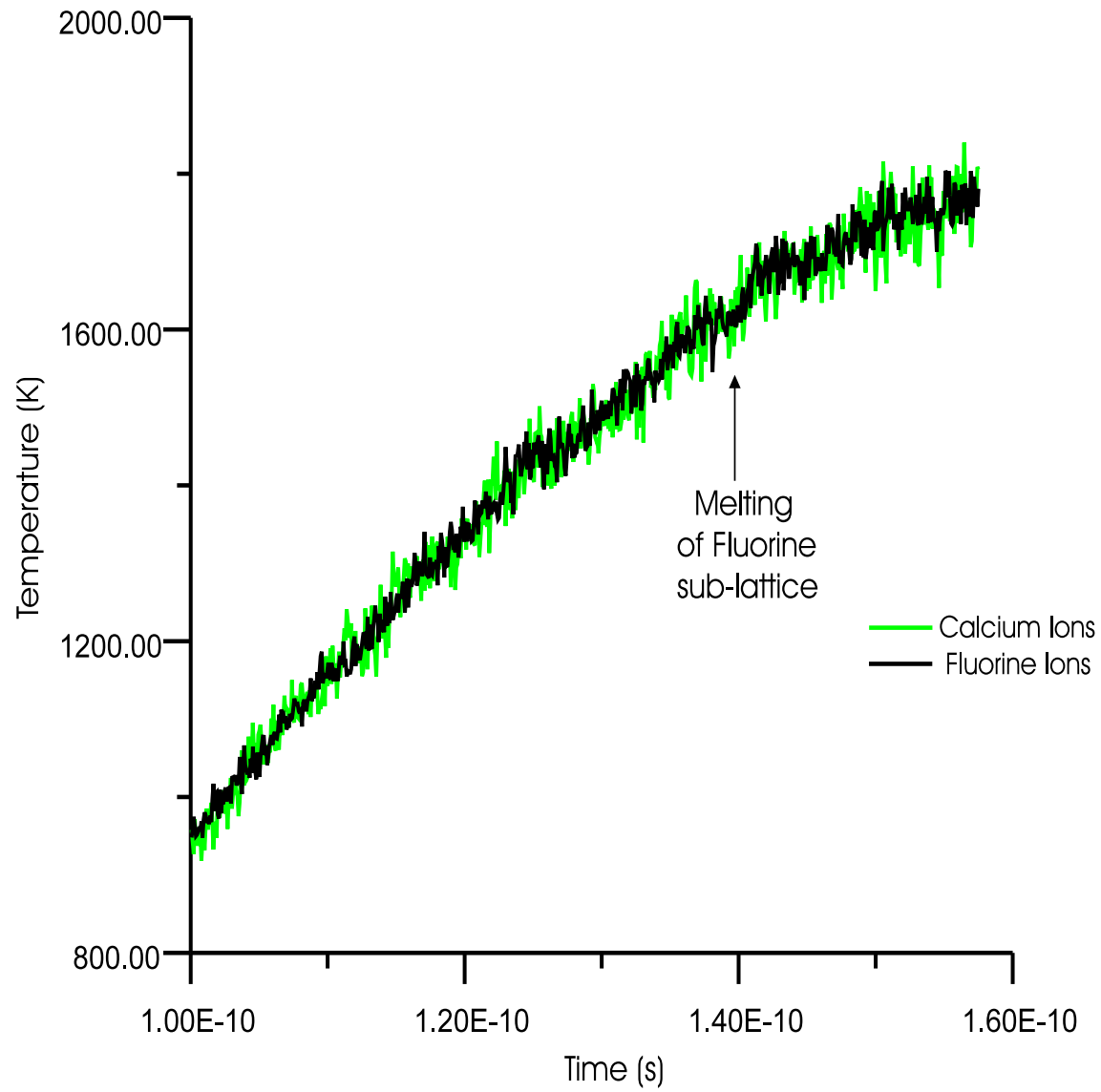


Figure 7.20: Heating history of the cluster

that the cluster is essentially constructed by cleaving a larger crystal. Although this method of calculating bond lengths is affected by both bulk and surface phenomena, it is particularly useful in that this is exactly the method used to calculate bond lengths from real diffraction patterns.

55.0ps The FT for the relaxed cluster are shown in Figures 7.23 and 7.22. The fluorine FT (Figure 7.23) has lost its ‘smearing’ and the symmetric ‘halos’ formed around the (100) reflections have disappeared. Both of these effects are a result of surface relaxation. Such relaxation is primarily seen at the surfaces of the cluster, especially on the type III surfaces (Figure 7.18 - Bottom). The $\text{F}^- - \text{F}^-$ and $\text{Ca}^{2+} - \text{Ca}^{2+}$ bond lengths show no change, within the limits of the method of calculation, after the cluster has relaxed.

70.0ps This is a snapshot of the cluster after its second equilibration at 300K. The FT’s of the species show very little change implying that the higher temperature equilibration has had very little effect on the degree of order (Figures 7.25 and 7.26). In general, the cluster at ambient temperatures shows very little difference from that at 10K. This would be expected considering that the cluster is still at a temperature where the quasi-harmonic approximation is still valid.

100.0ps The cluster is at approximately 1000K. The fluorine FT shows evidence of increased thermal vibrations; more diffuse intensity is evident and the (100) reflections have begun to broaden (Figure 7.28). Surprisingly, the calcium FT shows very little change (Figure 7.29), however the FT’s do indicate the lattice has expanded; the $\text{Ca}^{2+} - \text{Ca}^{2+}$ distance has risen to 5.55\AA (a 1.6% increase), the $\text{F}^- - \text{F}^-$ length has

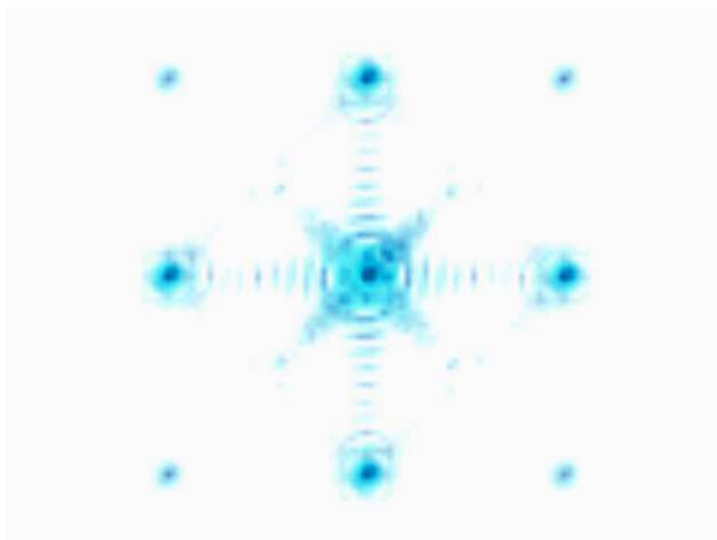


Figure 7.21: Fluorine Fourier transform at 0.0ps

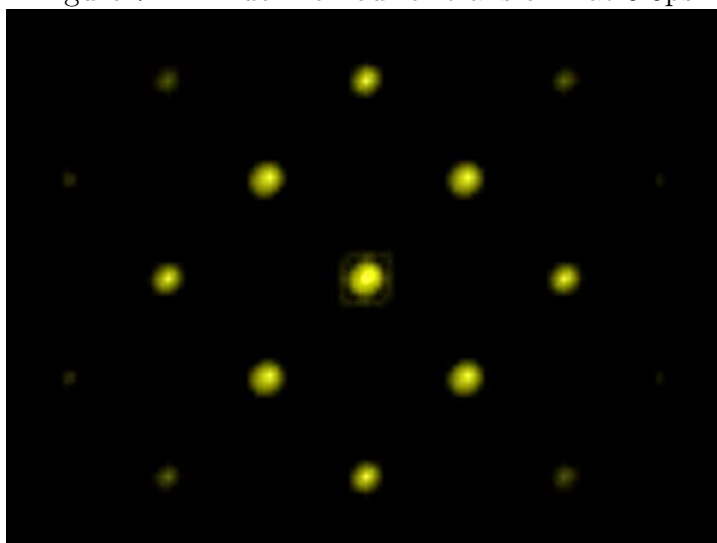


Figure 7.22: Calcium Fourier transform at 0.0ps

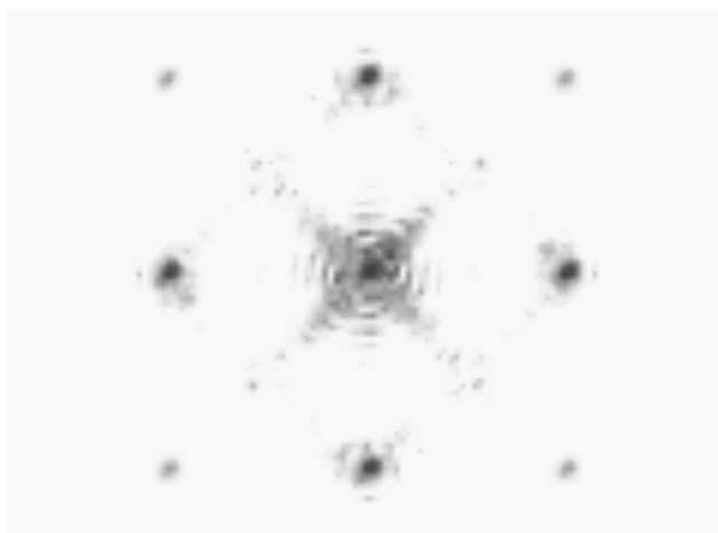


Figure 7.23: Fluorine Fourier transform at 50.0ps

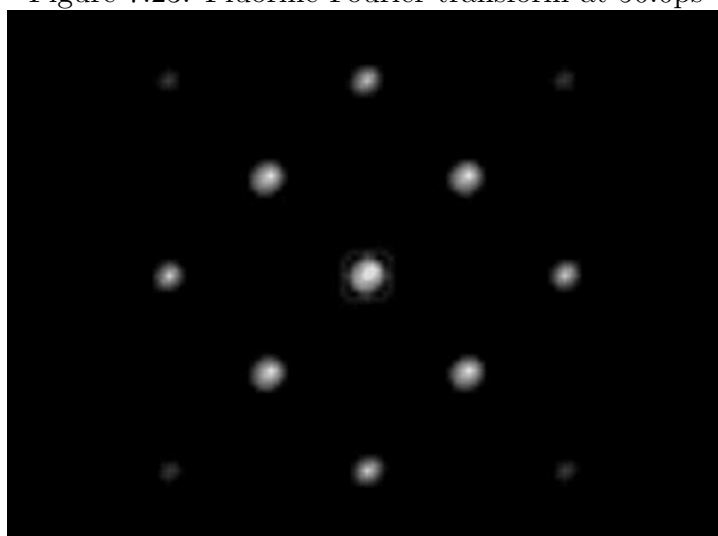


Figure 7.24: Calcium Fourier transform at 50.0ps

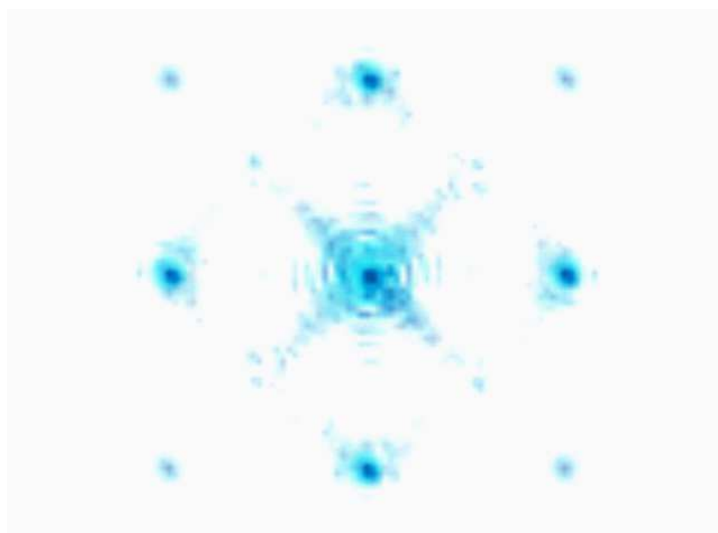


Figure 7.25: Fluorine Fourier transform at 70.0ps

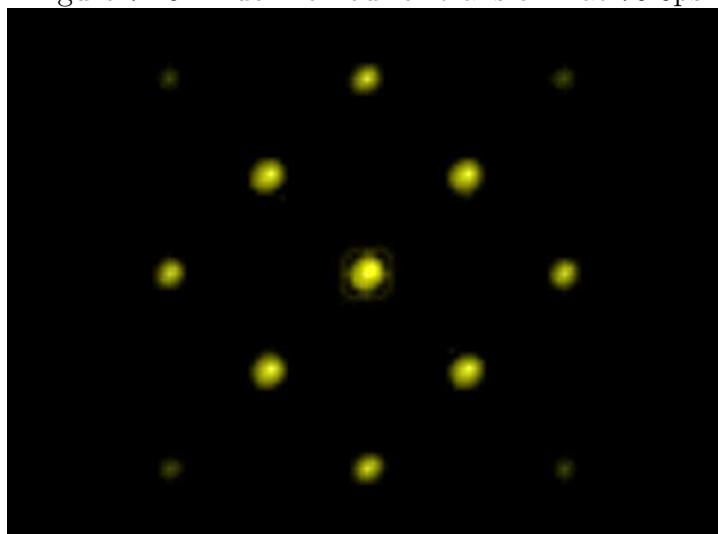


Figure 7.26: Calcium Fourier transform at 70.0ps

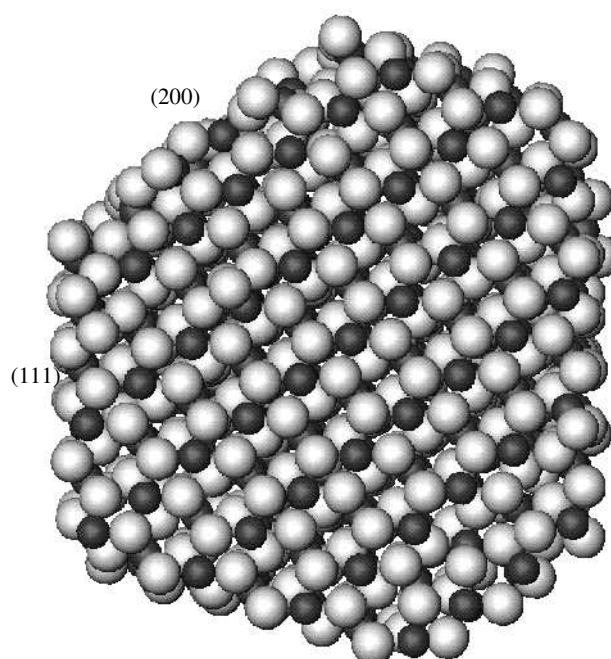


Figure 7.27: Atomic cross section at 70.0ps

increased by a similar amount to 2.78\AA . These greater amplitudes of vibration can be observed on the atomic snapshot (Figure 7.30) which shows large spaces between some of the atoms. The cluster also shows evidence of anion Frenkel defects. The main areas of disorder occur where the atoms have a lower coordination, such as near surfaces and corners of the cluster; the central part of the crystallite remains relatively unaffected.

120.0ps At this time, the lattice still shows a surprisingly high degree of order with both FT's showing sharp well defined reflections (Figure 7.31 and 7.32), even though the temperature is at 80% of the melting point, $\approx 1300\text{K}$. Figure 7.31 shows that the F^- ions are vibrating at a larger amplitude as the diffuse scatter from thermal effects become even more pronounced; the corresponding $\text{F}^- - \text{F}^-$ bond distance is

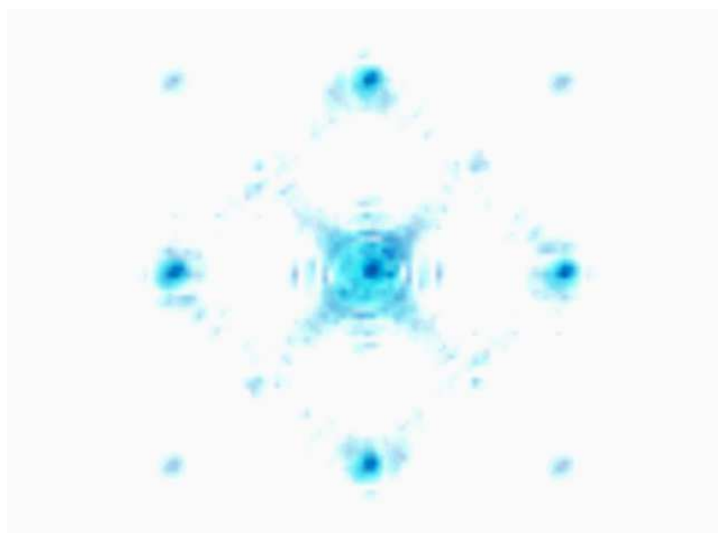


Figure 7.28: Fluorine Fourier transform at 100.0ps

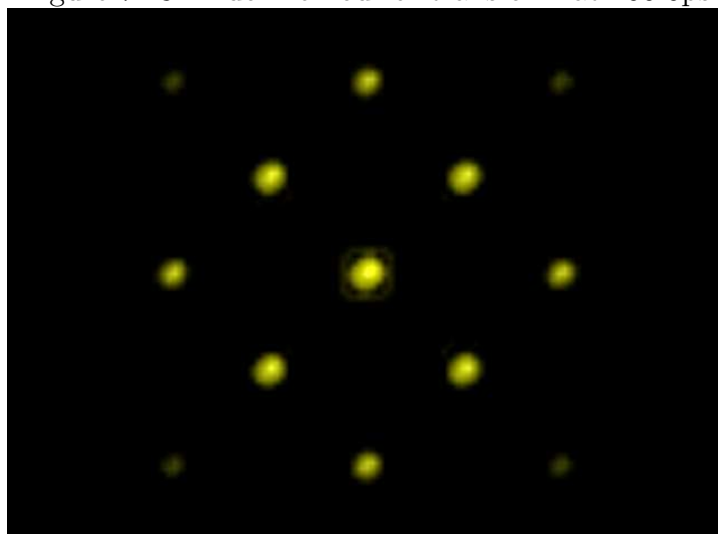


Figure 7.29: Calcium Fourier transform at 100.0ps

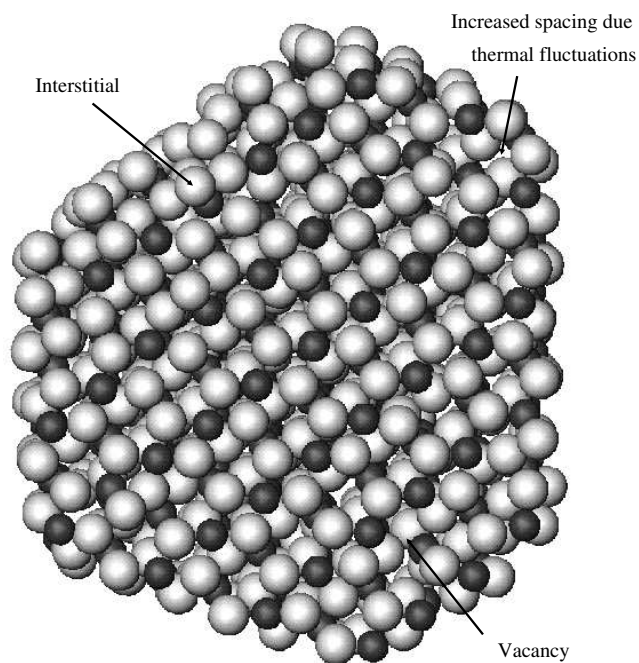


Figure 7.30: Atomic cross section at 100.0ps

2.80\AA (2.5% larger). The cluster shows well defined faces (Figure 7.33), however the spacing between the atoms in the surface layers has increased, implying that thermal vibrations are much larger at the surface. Additionally more anion vacancies and interstitial atoms are discernible implying the number of Frenkel defects is increasing with temperature as would be expected.

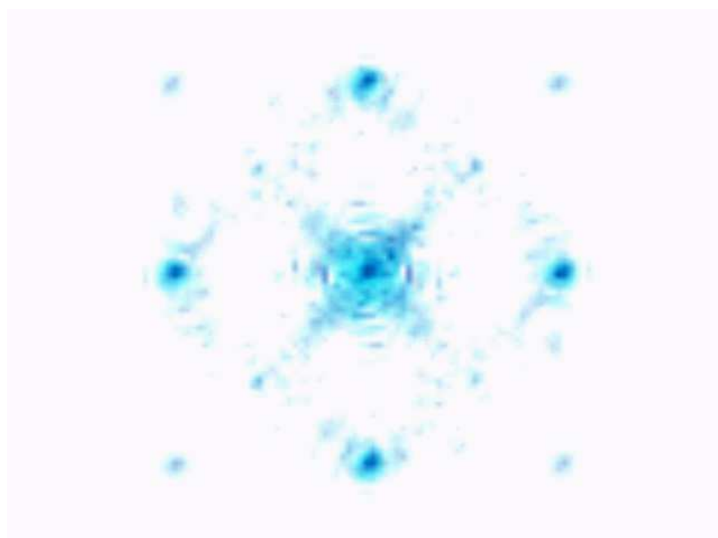


Figure 7.31: Fluorine Fourier transform at 120.0ps

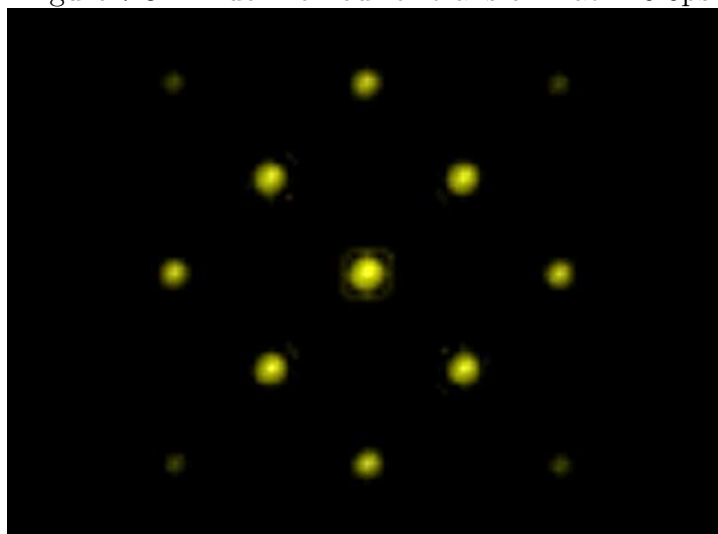


Figure 7.32: Calcium Fourier transform at 120.0ps

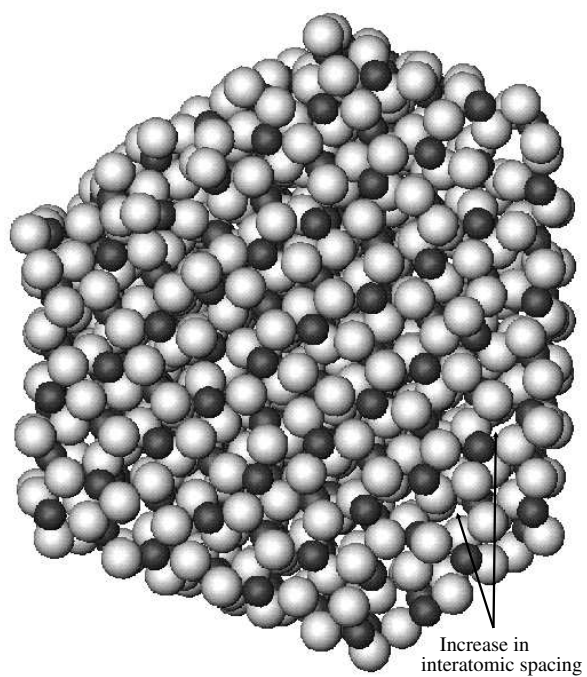


Figure 7.33: Atomic cross section at 120.0ps

131.0-140.5ps The fluorine sub-lattice, shows the first signs of melting at approximately 131.0ps (1500K). The FT indicates (Figure 7.34) a significant increase in the amount of disorder, characterised by an increase in diffuse scatter; the bond distance is now 2.82Å. However the sharp (100) and (110) reflections still remain. Nevertheless from Figure 7.35, it is clear that the most disordered regions are still concentrated at the surfaces of the cluster, particularly at the type III (200) surfaces. Figure 7.36 shows the FT of the cluster at 135.0ps, the fluorine sub-lattice has become almost amorphous. However, the (100) and (110) reflections are still fairly discernible.

The sub-lattice has essentially melted by 140.5ps (1650K) with the FT being completely amorphous (Figure 7.37). However, the Ca^{2+} sub lattice still show some order at this temperature (Figure 7.38). Nevertheless, the (220) reflections are relatively weak and the bond distance has increased by approximately 4.6% to 5.71Å. Figure 7.39 adds weight to the FT observations, the fluorine sub-lattice is seen to be almost completely disordered, except for possibly some of the anions in the centre. The calcium ions, on the other hand, still remain relatively ordered over a wider area in the cluster interior.

This effect of melting is also seen in Figures 7.19 and 7.20, where there is a distinct drop in the temperature of the cluster corresponding to the latent heat of melting. No doubt, in a larger cluster such a temperature drop would be more distinct as the thermal fluctuations would be smaller.

152.5-156.0ps In comparison to the F^- lattice the melting of the calcium sub-lattice occurs over a much shorter time and temperature scale. The calcium FT (Figure 7.40) at 1700K (152.5ps) shows a weakening of the (200) and (111) reflections, and the complete disappearance of the (220) reflections. In addition, diffuse scattering

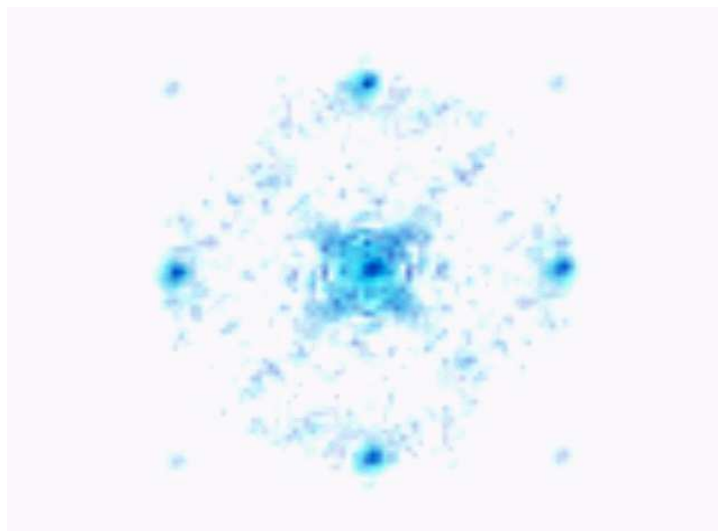


Figure 7.34: Fluorine Fourier transform at 131.0ps

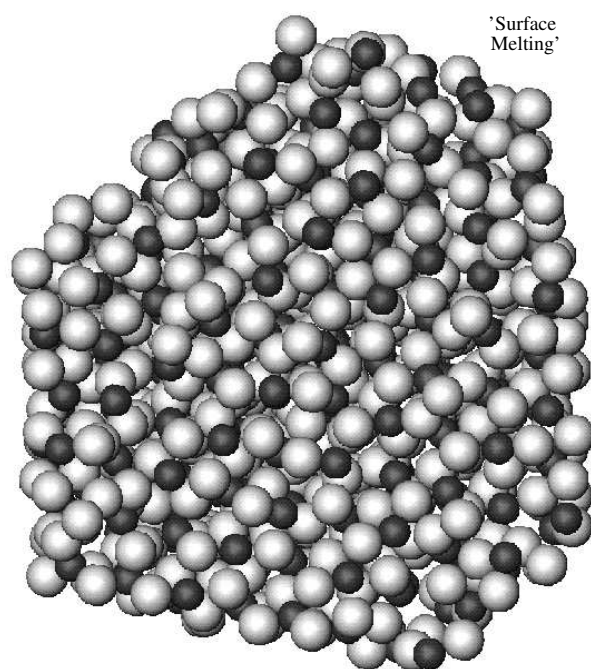


Figure 7.35: Atomic cross section at 131.0ps

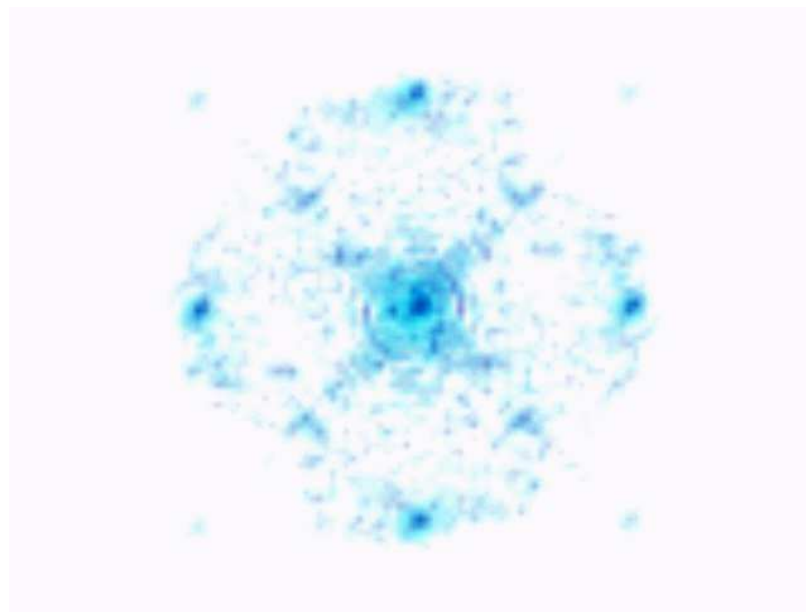


Figure 7.36: Fluorine Fourier transform at 135.0ps

due to thermal effects has become visible. From the cross section (Figure 7.41), it seems that the remaining order is concentrated at the centre of the lattice; the Ca^{2+} ions at the surface have become very disordered. Approximately 4.5ps later, (Figure 7.42 and 7.43) the sub-lattice has completely melted. The melting point of 1750K is slightly higher than the accepted melting point for CaF_2 , of 1696K [132]. However given that the temperature fluctuations in the present work are of the order of 80K, the experimental value is well within the uncertainty of the calculated melting point.

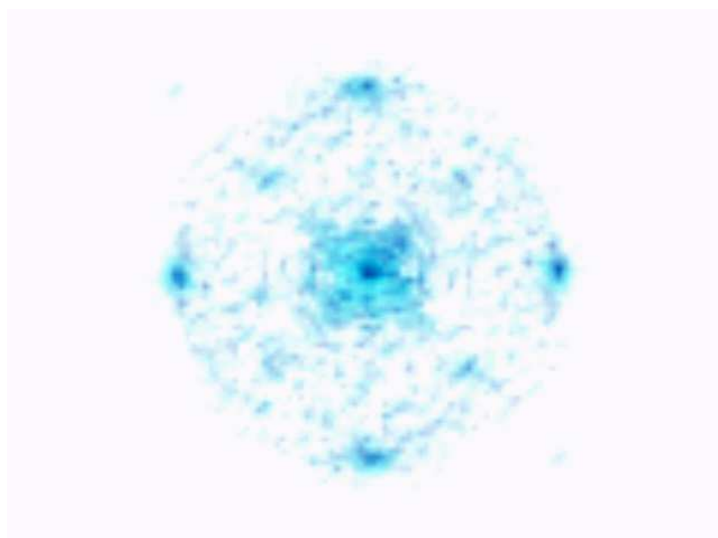


Figure 7.37: Fluorine Fourier transform at 140.5ps

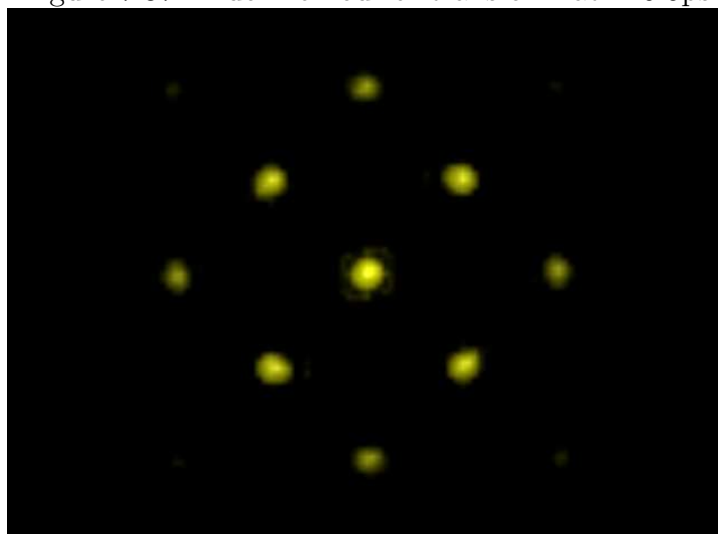


Figure 7.38: Calcium Fourier transform at 140.5ps

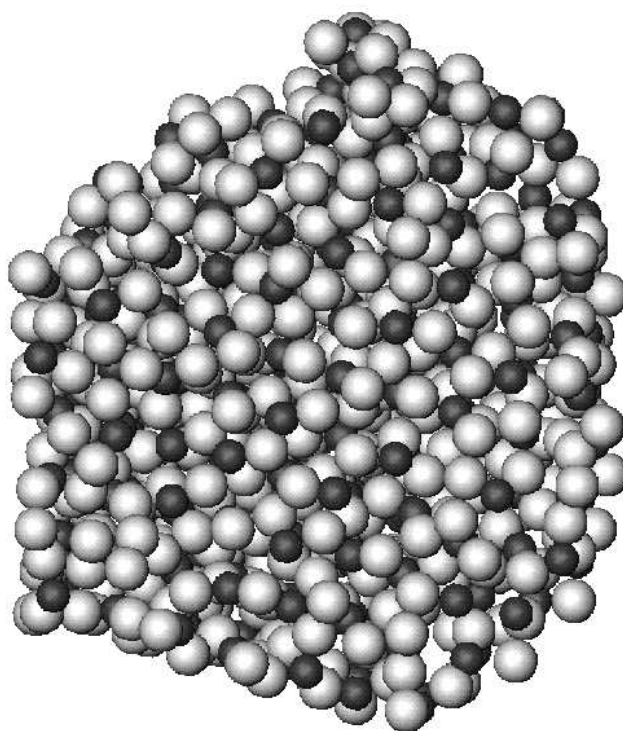


Figure 7.39: Atomic cross section at 140.5ps

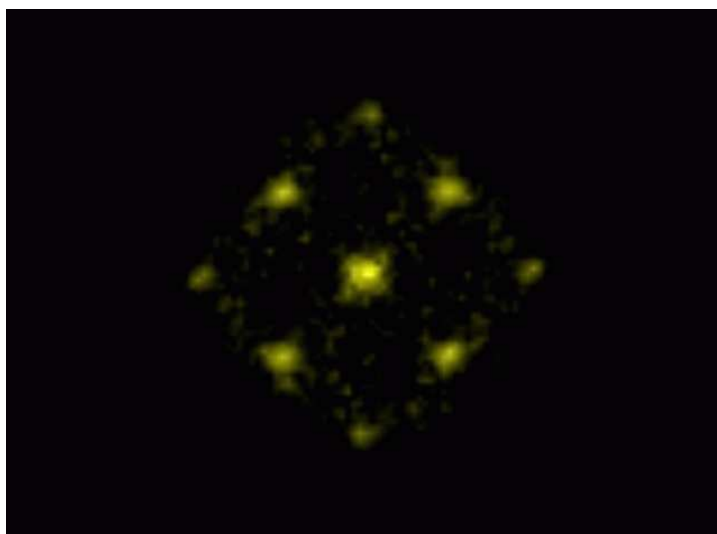


Figure 7.40: Calcium Fourier transform at 152.5ps

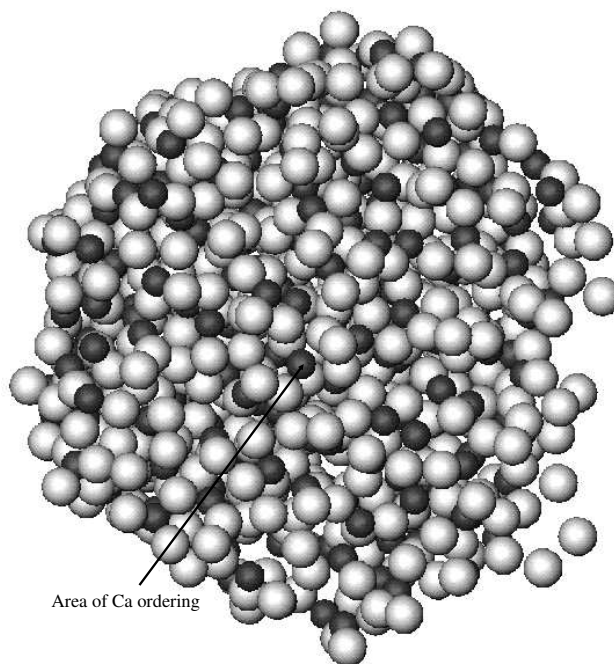


Figure 7.41: Atomic cross section at 152.5ps

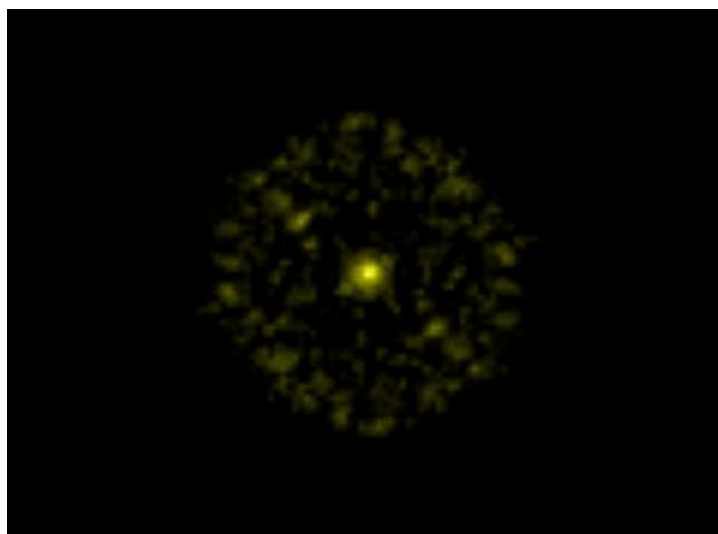


Figure 7.42: Calcium Fourier transform at 156.0ps

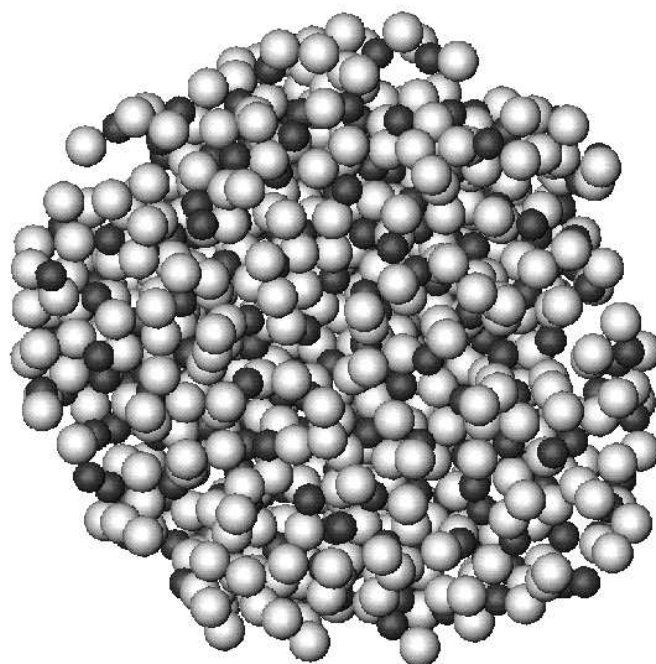


Figure 7.43: Atomic cross section at 156.0ps

7.5 The cooling of the 1665 atom cluster

Several attempts were made at re-crystallising the melted cluster. Cooling was carried out on clusters which had been equilibrated in the molten state using three different times so as to assess the effect of equilibration time on the re-crystallisation. In addition, different cooling rates were also used, in order to monitor the effect of this variable on the resulting cluster structure. The following figures show the FT's of the fluorine and calcium sub-lattices and graphs of the $\ln \{ \text{diffusion coefficients} \}$ as a function of reciprocal temperature for the different runs (see Table 7.3 for an index), i.e. $\ln(D_\alpha)$ vs. $1/T$. Information on the degree of ordering in the system can be determined from the FT's. The solidification of the clusters was also monitored by the graphs of $\ln(D_\alpha)$ vs. $1/T$.

The systems were cooled to 900K. In the majority of cases the clusters form glassy solids (Run No's 1 - 4 & 6). The graphs of $\ln(D_\alpha)$ vs. $1/T$ show no change in gradient implying that crystallisation does not occur and the FTs show no signs of order. These results seem to be in agreement with the results of previous MD studies [133, 134, 135] where the systems remained as supercooled liquids over a large temperature range, before forming glassy solids. Table 7.4 shows the calculated activation energies for migration of the different runs. In general, the activation energies for fluorine and calcium show no great difference. In addition, the values for both species are small, again indicating that the cluster is acting as a liquid.

The slowest cooling rate was used for Run No. 5. In this case, the calcium FT (Figure 7.56) shows some evidence of ordering with the presence of well defined reflections. However, no such reflections were observed for the corresponding fluorine FT. Thus, it can be concluded that some ordering can result from using very slow (on

the atomic time scale) cooling rates. Further work must be carried out using slower cooling rates and possibly bigger clusters to see if the fluorine sub-lattice can also be persuaded to crystallise.

Run No.	Eqm. Time (ps)	Cooling Rate Ks^{-1}	Figure
1	6.5	5.0×10^{13}	7.44-7.46
2	6.5	2.5×10^{13}	7.47-7.49
3	35.7	5.0×10^{13}	7.50-7.52
4	35.7	2.5×10^{13}	7.53-7.55
5	35.7	2.5×10^{12}	7.56-7.58
6	60.0	5.0×10^{13}	7.59-7.61

Table 7.3: Cooling rates and equilibration times for the different runs

Run No	Activation Energy (eV)	
	Ca^{2+}	F^-
1	0.36	0.35
2	0.47	0.38
3	0.52	0.49
4	0.22	0.39
5	0.50	0.39
6	0.43	0.36

Table 7.4: Calculated activation energies

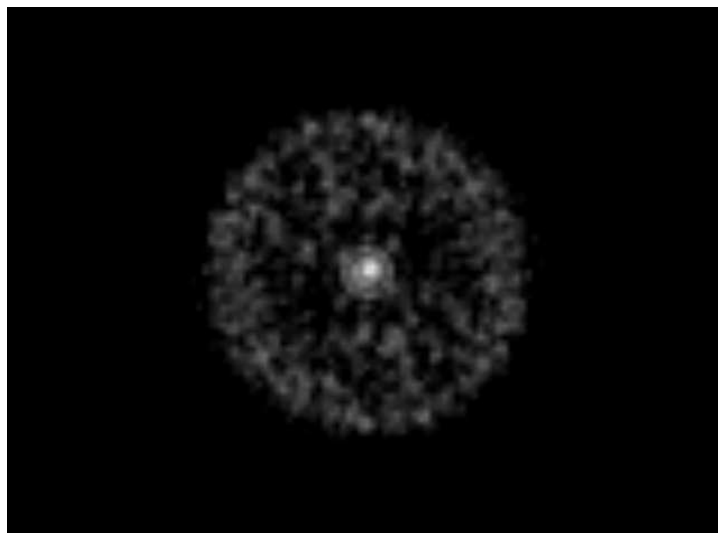


Figure 7.44: Calcium FT - Run No. 1

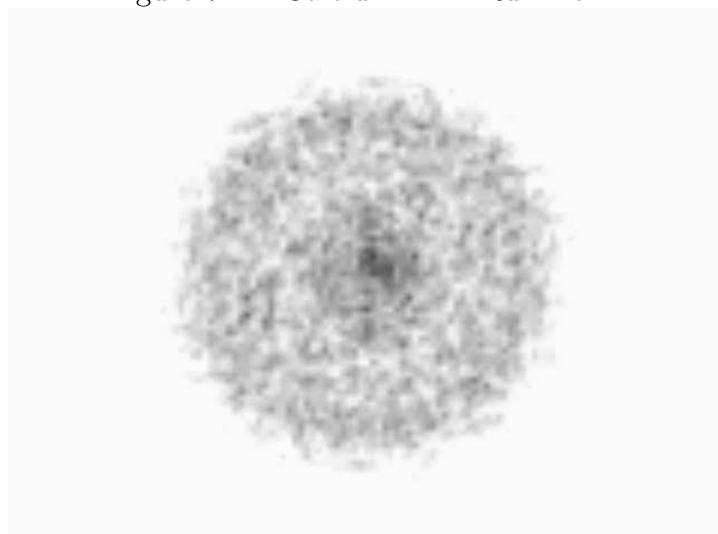
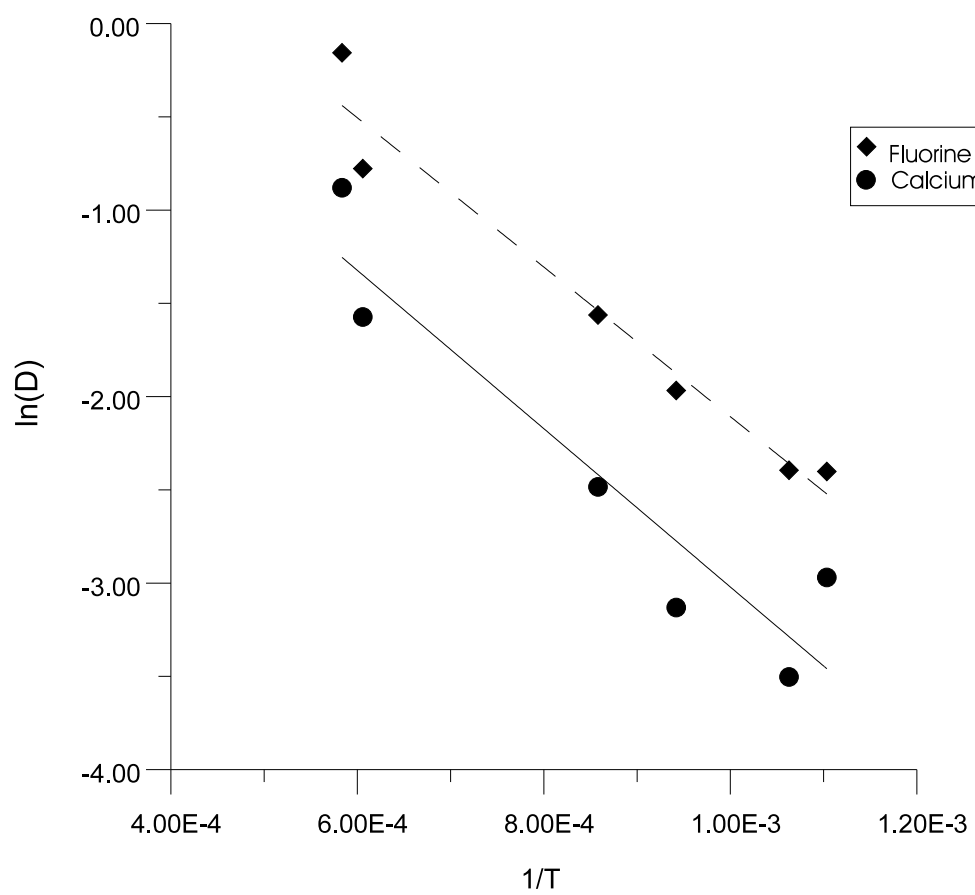


Figure 7.45: Fluorine FT - Run No. 1

Figure 7.46: $\ln(D)$ vs. $1/T$ - Run No. 1

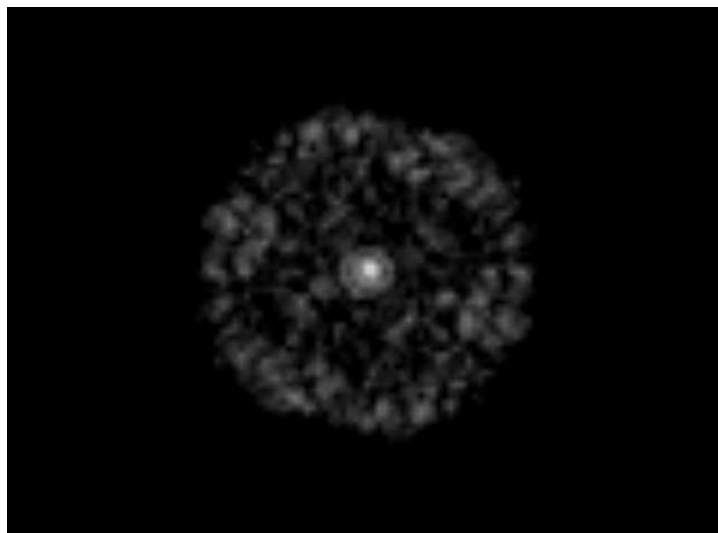
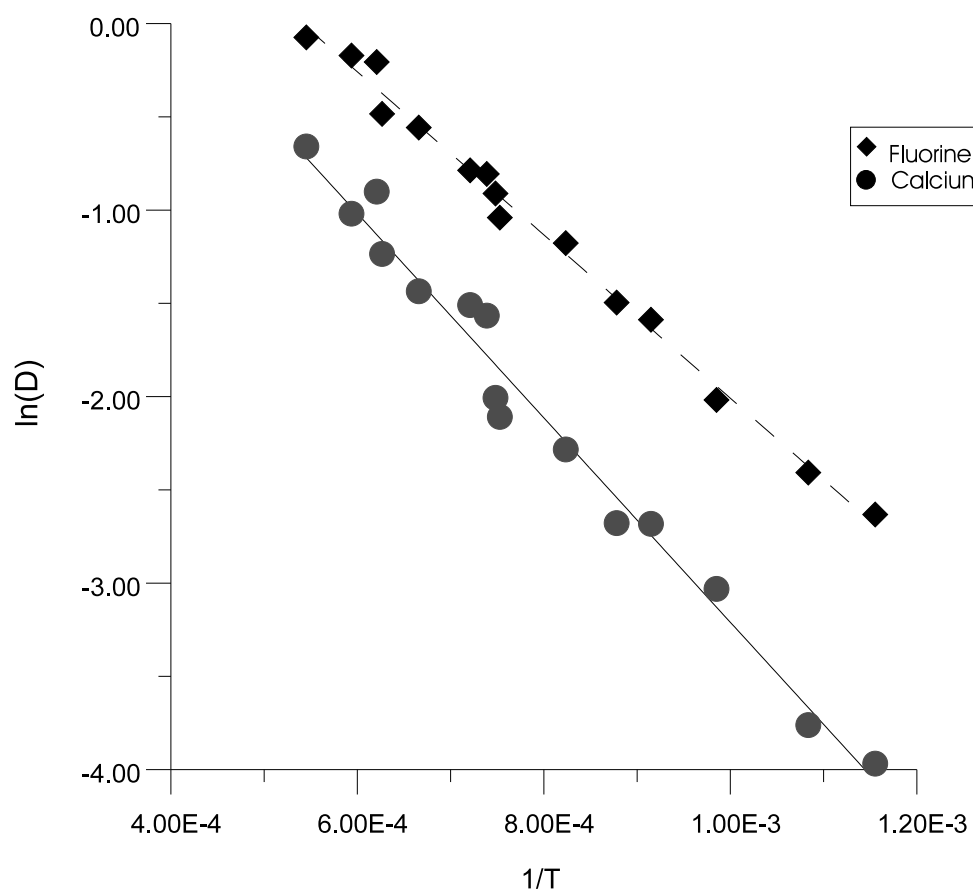


Figure 7.47: Calcium FT - Run No. 2



Figure 7.48: Fluorine FT - Run No. 2

Figure 7.49: $\ln(D)$ vs. $1/T$ - Run No. 2

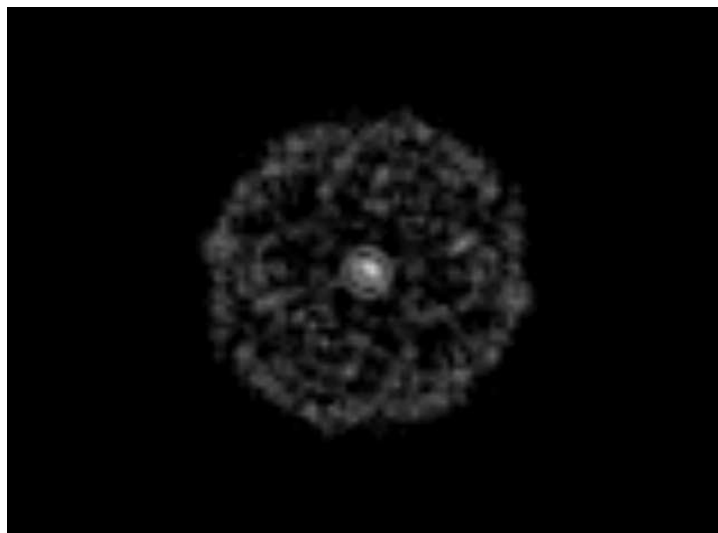


Figure 7.50: Calcium FT - Run No. 3



Figure 7.51: Fluorine FT - Run No. 3

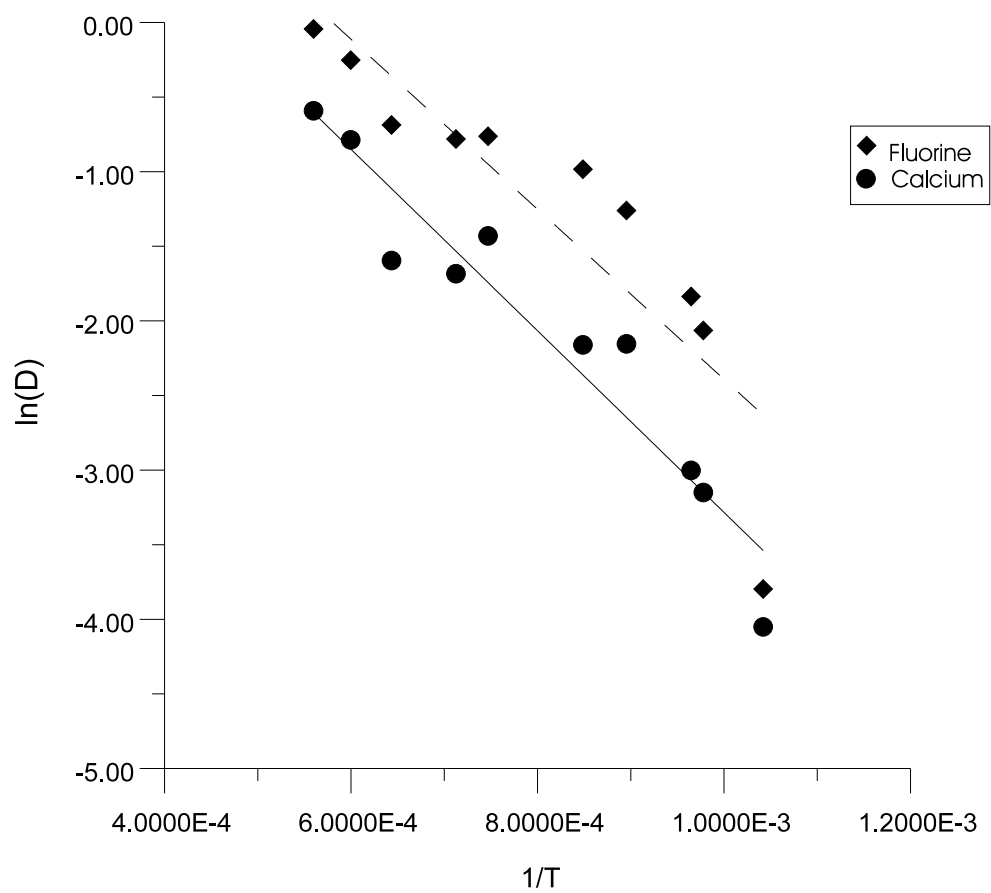


Figure 7.52: The diffusion coefficient as a function of temperature - Run No. 3

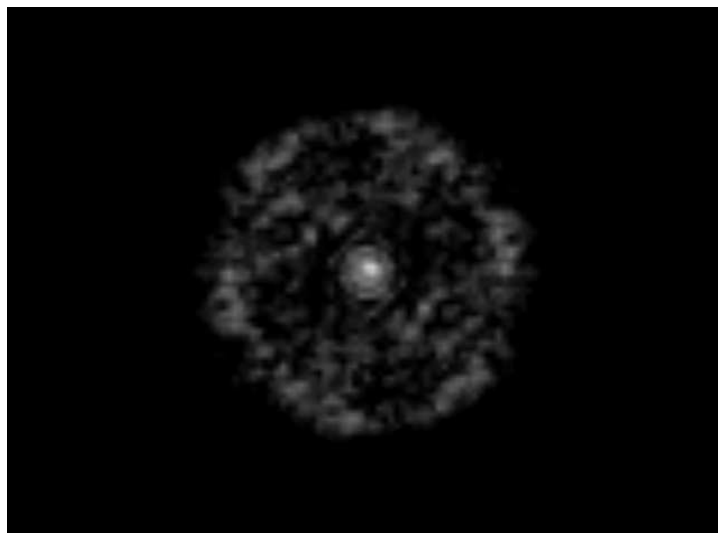


Figure 7.53: Calcium FT - Run No. 4

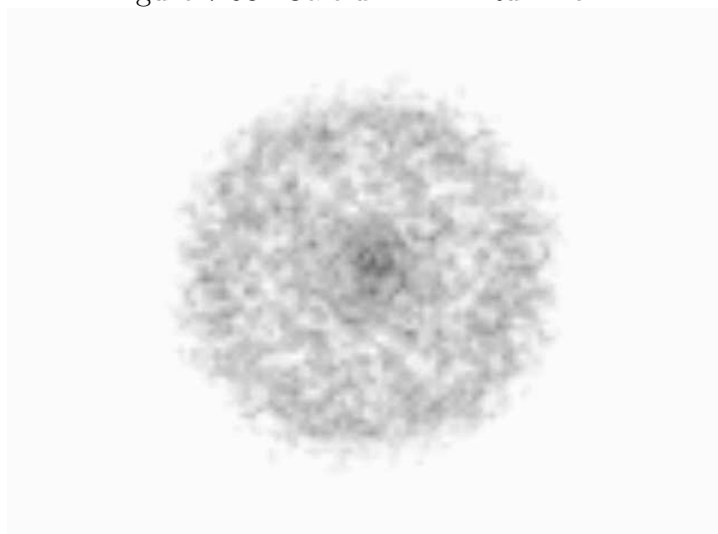
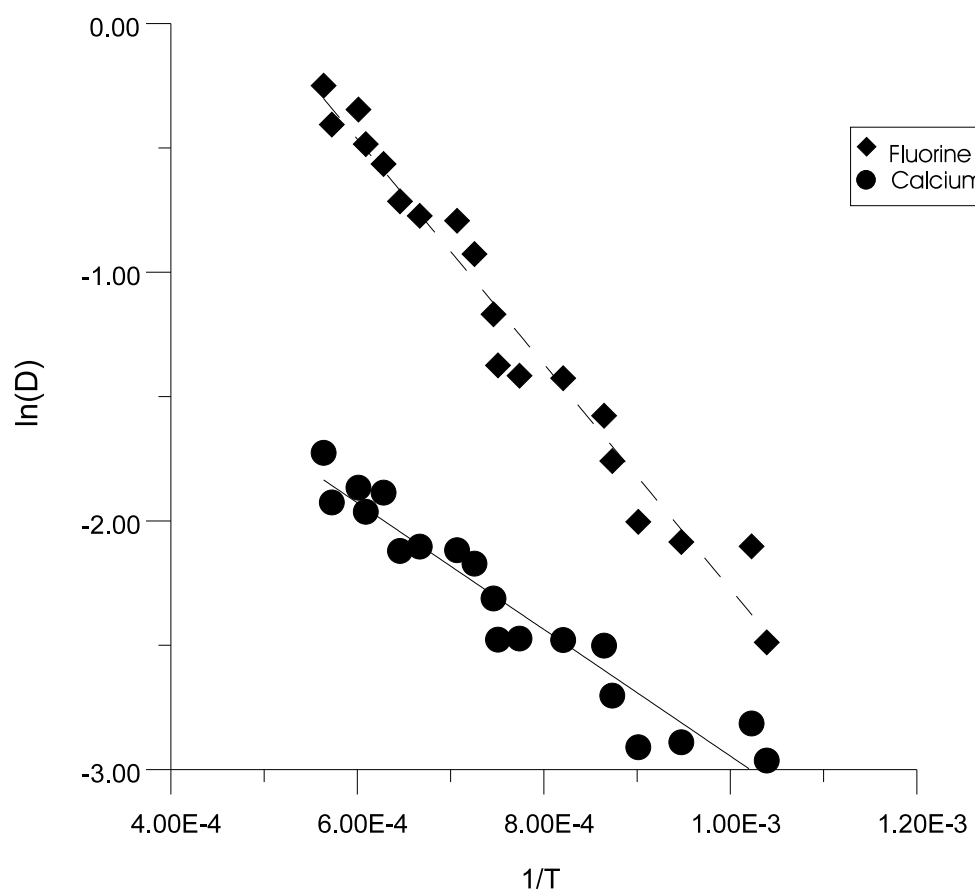


Figure 7.54: Fluorine FT - Run No. 4

Figure 7.55: $\ln(D)$ vs. $1/T$ - Run No. 4

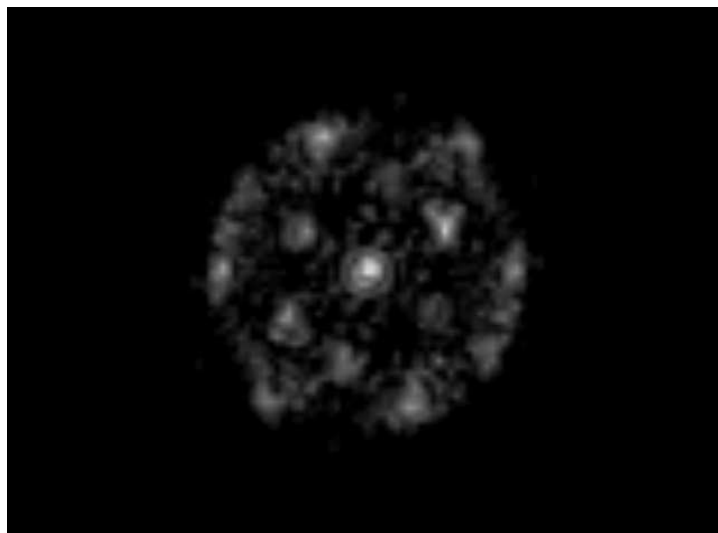


Figure 7.56: Calcium FT - Run No. 5

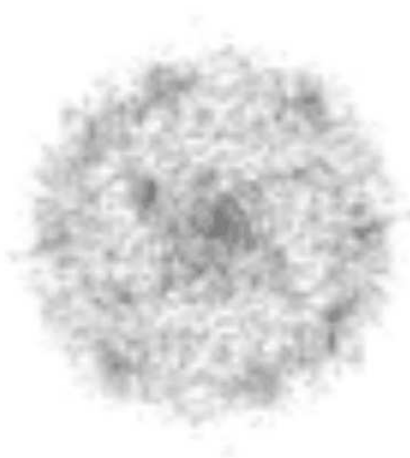


Figure 7.57: Fluorine FT - Run No. 5

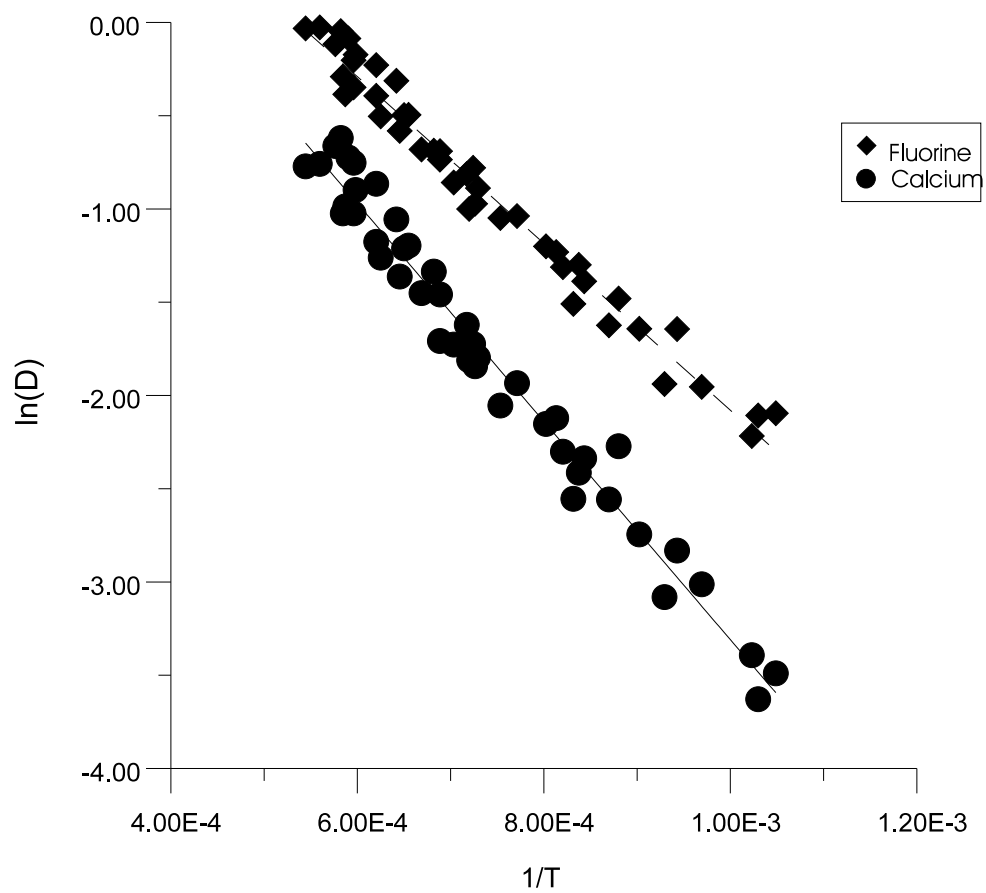


Figure 7.58: $\ln(D)$ vs. $1/T$ - Run No. 5

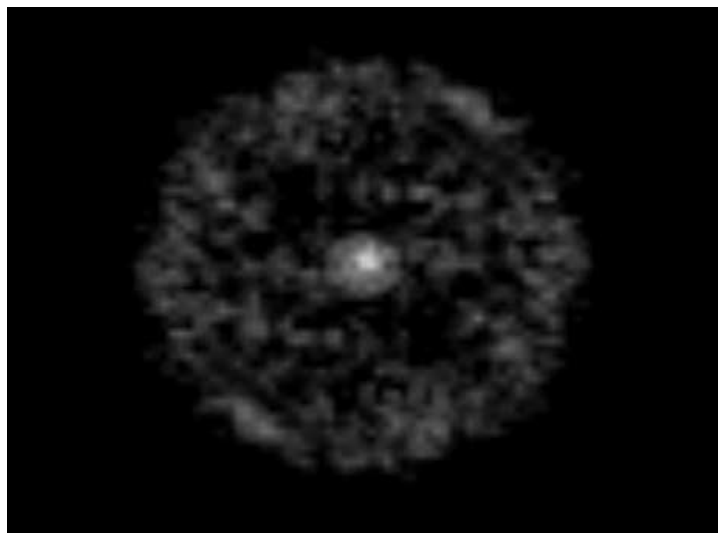


Figure 7.59: Calcium FT - Run No. 6

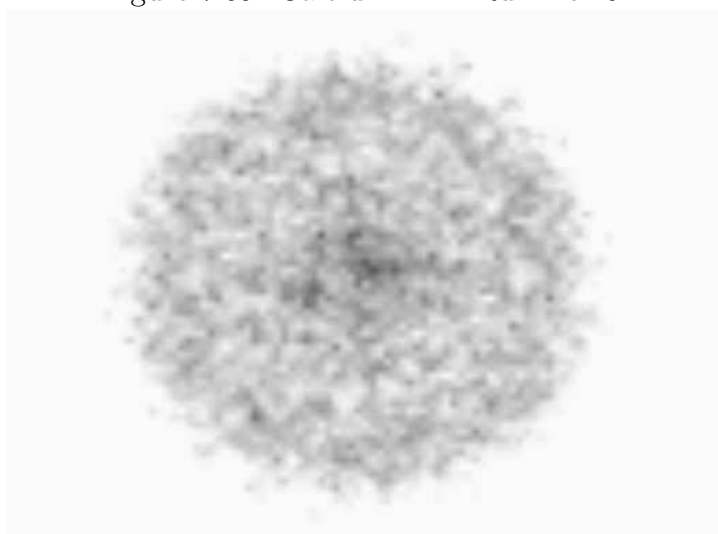
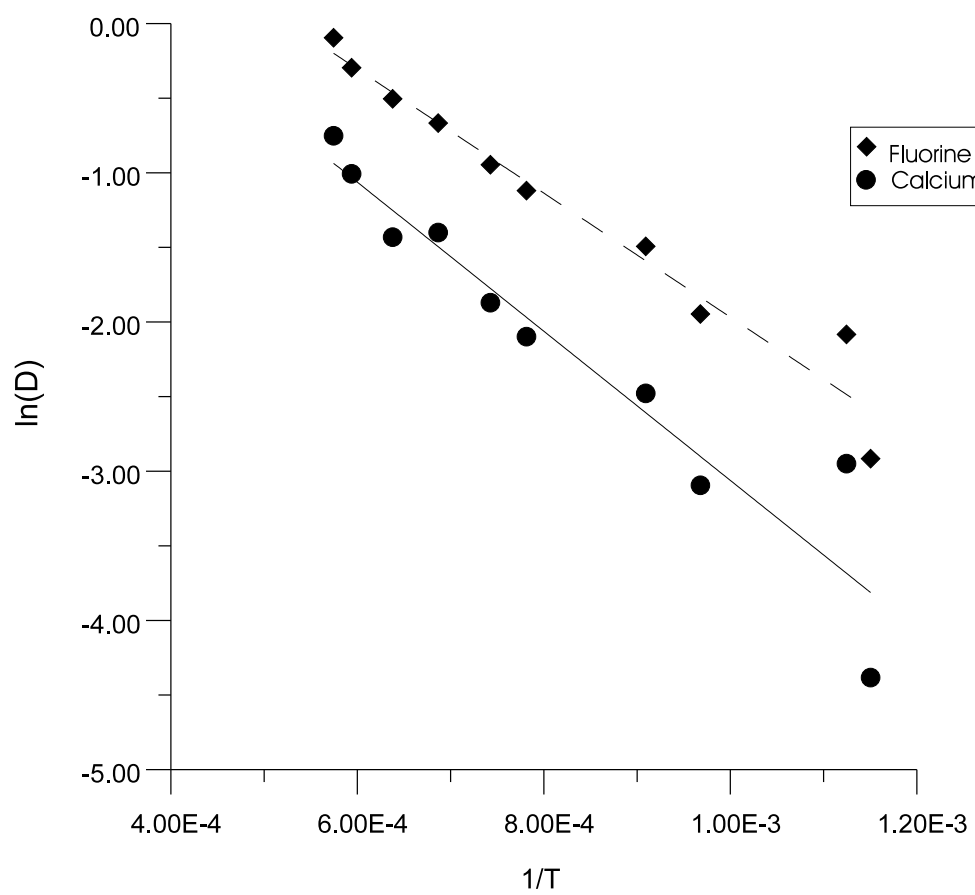


Figure 7.60: Fluorine FT - Run No. 6

Figure 7.61: $\ln(D)$ vs. $1/T$ - Run No. 6

7.6 Summary

MD simulations were carried out on two different sized nano-crystals of CaF_2 . The surface structures of these clusters were examined after a suitable equilibration time and compared with infinite 2D surface simulations. The relaxation of the clusters is analogous to the 2D static simulations, however the smaller cluster shows an extreme relaxation at the edges and points where the faces meet, thus forming a more spherical cluster. The atomic arrangement of the type III faces in both clusters, after equilibration, is particularly important, in that it gives rise to a similar structure to that assumed to when carrying out static calculations of infinite surfaces.

Studies of melting and crystallisation were also carried on the smaller cluster. It was found that anion Frenkel defects form at approximately 1000K and that the fluorine sub-lattice melts over a much longer time scale ($\approx 10\text{ps}$) and temperature range ($\approx 150\text{K}$) than the calcium sub-lattice. From the FT's it was shown that the calcium sub-lattice remains relatively ordered until just below the melting point, when it melts rapidly over a very short time scale (4.5ps). Several attempts were made to re-crystallise the melted cluster using a range of equilibration times and cooling rates. The presence of ordering was seen in the run using the slowest cooling rate (Run No. 5), however, in all other cases the systems formed a glassy solid.